

## **13. TITAN-I SAFETY DESIGN AND RADIOACTIVE-WASTE DISPOSAL**

Clement P. C. Wong  
Edward T. Cheng  
Charles G. Hoot

Steven P. Grotz  
Robert W. Conn  
Farrokh Najmabadi  
Kenneth R. Schultz

James P. Blanchard  
Richard L. Creedon  
Shahram Sharafat

## Contents

|         |   |       |
|---------|---|-------|
| 13.1.   | INTRODUCTION . . . . .  | 13-1  |
| 13.2.   | SAFETY-DESIGN GOALS . . . . .                                   | 13-1  |
| 13.3.   | SAFETY-DESIGN FEATURES . . . . .                                | 13-5  |
| 13.3.1. | Design Guidelines . . . . .                                     | 13-5  |
| 13.3.2. | Material Selection . . . . .                                    | 13-6  |
| 13.3.3. | Configuration and Lithium-Drain-Tank Design . . . . .           | 13-8  |
| 13.3.4. | Confinement-Building Cover Gas . . . . .                        | 13-11 |
| 13.3.5. | Tritium Issues . . . . .  | 13-13 |
| 13.4.   | LOSS-OF-FLOW & LOSS-OF-COOLANT ACCIDENTS . . . . .              | 13-14 |
| 13.4.1. | Accident Models . . . . .                                       | 13-15 |
| 13.4.2. | Thermal Response to LOCA and LOFA . . . . .                     | 13-20 |
| 13.4.3. | Elevated-Temperature Creep Rupture . . . . .                    | 13-25 |
| 13.4.4. | Conclusions . . . . .   | 13-32 |
| 13.5.   | LITHIUM-FIRE ACCIDENTS . . . . .                                | 13-32 |
| 13.6.   | PLASMA ACCIDENTS . . . . .                                      | 13-37 |
| 13.6.1. | Shutdown Procedures . . . . .                                   | 13-39 |
| 13.7.   | RADIOACTIVE-WASTE DISPOSAL . . . . .                            | 13-40 |
| 13.7.1. | Radioactive-Waste-Disposal Issues . . . . .                     | 13-40 |
| 13.7.2. | Radioactive-Waste-Disposal Ratings of TITAN-I Reactor . . . . . | 13-41 |
| 13.7.3. | Conclusions . . . . .   | 13-45 |
| 13.8.   | SUMMARY AND CONCLUSIONS . . . . .                               | 13-45 |
|         | REFERENCES . . . . .  | 13-48 |

## **13. TITAN-I SAFETY DESIGN AND RADIOACTIVE-WASTE DISPOSAL**

### **13.1. INTRODUCTION**

Strong emphasis has been given to safety engineering in the TITAN study. Instead of an add-on safety design and analysis task, the safety activity was incorporated into the process of design selection and integration at the beginning of the study. The safety-design objectives of the TITAN-I design are: (1) to satisfy all safety-design criteria as specified by the U. S. Nuclear Regulatory Commission on accidental releases, occupational doses, and routine effluents and (2) to aim for the best possible level of passive safety assurance.

This section presents the safety design and evaluations of the TITAN-I reactor. The safety design goals for the TITAN reactors are discussed in Section 13.2 and the safety-design features are reviewed in Section 13.3. Safety analyses for the TITAN-I design are reported in Section 13.4 for loss-of-flow and loss-of-coolant accidents in the fusion power core, in Section 13.5 for lithium fires, and in Section 13.6 for plasma-related accidents. Section 13.7 describes the radioactive-waste-disposal issues and ratings for the TITAN-I design. A summary of the TITAN-I safety design and analysis is given in Section 13.8.

### **13.2. SAFETY-DESIGN GOALS**

Two main objectives have guided the TITAN safety design: (1) to satisfy all safety-design criteria as specified by the U. S. Nuclear Regulatory Commission (U. S. – NRC) on accidental releases, occupational doses, and routine effluents; and (2) to aim for the best possible level of safety assurance.

Although the accident scenarios and classification systems developed by the U. S. fission industry may not apply directly to fusion reactors, the dose guidelines used by the fission industry will probably either be directly applicable or serve as useful references in defining the radiological safety requirements for fusion-reactor designs. The U. S. – NRC regulations covering fission reactors are described in the Code of Federal Regulations in Sections:

- 10CFR20 – Standards for Protection Against Radiation [1],
- 10CFR50 – Domestic Licensing of Production and Utilization Facilities [2],
- 10CFR100 – Reactor Site Criteria [3],
- 10CFR61 – Licensing Requirements for Land Disposal of Radioactive Waste [1].

Table 13.2-I describes the present industry guidelines [4] for satisfying the regulations and the dose-limit values are shown in Table 13.2-II. These NRC regulations define the maximum dose limits and releases of radioactivity during routine and anticipated

**Table 13.2-I.**

**PRESENT INDUSTRY GUIDELINES ON DOSE EXPOSURE [4]**

| Frequency of Occurrence<br>per Reactor Year, $F$ <sup>(a)</sup> | Off-Site Dose                      |
|---|------------------------------------|
| Planned operations  | 10CFR50, Appendix I <sup>(b)</sup> |
| $F > 10^{-1}$   | 10CFR50, Appendix I <sup>(b)</sup> |
| $10^{-1} > F > 10^{-2}$   | 10% of 10CFR100 <sup>(c)</sup>     |
| $10^{-2} > F > 10^{-4}$   | 25% of 10CFR100 <sup>(c)</sup>     |
| $10^{-4} > F > 10^{-6}$   | 100% of 10CFR100 <sup>(c)</sup>    |

(a) Data compiled from fission-reactor license applications reviewed by the NRC.

(b) Dose objective of 10CFR50, Appendix I must be met for the summation of radioactive releases due to planned operations and the annual average of events with  $F \sim 0.1$ . Individual radionuclide concentration limits are given by 10CFR20, Appendix B [1].

(c) Dose limits during preliminary design and review are 80% of the maximum allowable whole body limit and 50% of the maximum allowable limits for all other doses [3].

**Table 13.2-II.**  
**REGULATORY DOSE LIMITS**

---

**10CFR20 – Routine Release [1]**

- Maximum permissible concentrations of radionuclides in air and water:
  - specified by individual isotopes for occupational and public areas
- Occupational exposure:
  - whole body or individual organs 5 rem/y
  - extremities 75 rem/y
  - skin 30 rem/y

**10CFR50, Appendix I (Public)<sup>(a)</sup> – Routine Release [2]**

- Gases:
  - total body 5 mrem/y
  - skin 15 mrem/y
- Liquids:
  - total body or any organ 5 mrem/y
  - total release per reactor (except tritium & dissolved gases) 5 Ci/y
- Particulates:
  - any organ 15 mrem/y
- As low as is reasonably achievable (ALARA):
  - cost/benefit guideline expenditure to reduce exposure 1000 \$/man-rem

**10CFR100 – Accidental Release [3]**

- Two-hour dose at site boundary, or dose during entire event at low population zone:
  - whole body 25 rem
  - thyroid 300 rem
  - bone, lung, and other organs<sup>(b)</sup> 150 rem

---

(a) The Department of Energy (DOE) recently proposed a limit of 100 mrem/y annual dose from all routine operations to the public near DOE facilities [5].

(b) Inferred from 10CFR100 intent [6].

operations (10CFR20 [1] and 10CFR50 [2]) and during severe hypothetical accidents (10CFR100 [3]). In general, these guidelines were based on the biological effect of a radioactive release and thus are independent of the source of the release. Therefore, even though the regulations frequently reference nuclides of importance to nuclear fission which will have no significance in fusion (*e.g.*, thyroid dose from  $^{131}\text{I}$ ), the intent of the guidelines remains valid.

Recently, four levels of safety assurance were proposed to facilitate the preliminary evaluation of different designs [7,8]. While these levels are neither precisely defined licensing criteria nor rules for formal safety evaluation, they do provide a relatively simple guide for designers who can use these definitions of different levels of safety to evaluate their designs or to improve on their safety features when appropriate. The following summarize the interpretation of these four levels of safety assurance as suggested by Piet [7] (also see Reference [8]).

*Level 1 – “Inherent safety.”* Safety is assured by inherent mechanisms of release limitation no matter what the accident sequence is. The radioactive inventories and material properties in such a reactor preclude a violation of release limits regardless of the reactor condition.

*Level 2 – “Large-scale passive-safety assurance.”* Safety is assured by passive mechanisms of release limitation as long as severe reconfiguration of large-scale geometry is avoided, and escalation to fatality-producing reconfigurations from less severe initiating events can plausibly be precluded by passive design features. In such a reactor, natural heat-transfer mechanisms suffice to keep temperatures below those needed, given the radioactivity inventory and material properties, to produce a violation of release limits unless the large-scale geometry is badly distorted.

*Level 3 – “Small-scale passive-safety assurance.”* Safety is assured by passive mechanisms of release limitation as long as severe violations of small-scale geometry, such as a large break in a major coolant pipe, are avoided, and escalation to fatality-capable violations from less severe initiating events can plausibly be precluded by passive design features. In such a reactor, sufficiency of natural heat-transfer mechanisms to keep temperatures low enough, given its radioactivity inventories and materials properties, to avoid a violation of release limits can only be assured while the coolant boundary is substantially intact.

*Level 4 – “Active safety assurance.”* There are credible initiating events that can only be prevented from escalating to site-boundary-release limit violations or reconfigurations by means of active safety systems. This is the conventional approach of add-on safety.

The public is adequately protected by all four levels of safety assurance. To understand the meaning of adequate protection of the public, the concept of safety assurance can be further strengthened in the context of probabilistic risk assessment. The risk-based safety goal for TITAN is that fusion accidents would not increase the individual cancer risk of the public by more than 0.1% of the prevailing risk. As a consequence of this goal, a site-boundary whole-body dose limit of 25 rem for accidental release for fission reactors (10CFR100 [3]) has been adopted.

### 13.3. SAFETY-DESIGN FEATURES

#### 13.3.1. Design Guidelines

The TITAN-I fusion power core (FPC) is cooled by liquid lithium. Four basic safety-design approaches were incorporated into the design:

1. Physical separation of potentially reactive materials, such as lithium, water, concrete, and air (*e.g.*, by using multiple physical barriers);
2. Minimization of the amount of induced radioactivities (*e.g.*, by using reduced-activation materials);
3. Reducing the maximum material temperature caused by decay afterheat (*e.g.*, by using low-afterheat materials and by providing thermally conducting paths from the front to the back of the blanket);
4. Minimization of the amount of vulnerable lithium coolant (*e.g.*, by using lithium drain tanks).

Based on these design approaches, the following guidelines were derived.

- Low-activation and low-afterheat materials and designs should be used wherever possible to minimize the amount of releasable radioactivity.
- Passive afterheat-removal designs should be emphasized (*e.g.*, use of conducting paths leading from the first wall to the back of the blanket, and natural circulation for transferring the afterheat energy to a heat sink).
- Passive safety features should be incorporated in the plasma-engineering design to reduce the impact of plasma accidents.

- The FPC should be located below grade to reduce the impact from earthquakes and above-ground accidental events (*e.g.*, aircraft crash).
- In order to avoid a complete loss-of-coolant accident from accidental drainage, primary-piping connections should be located above the FPC.
- The entire primary-coolant system should be enclosed within the confinement building (or buildings, depending on the detailed reactor layout), and the confinement building(s) should be filled with argon cover gas in order to reduce the probability of a lithium fire.
- Water should be excluded from the confinement building or vacuum vessel to prevent the probability of lithium-water reaction.
- The confinement-building floor should be covered with steel liner and the walls and ceiling should be sealed with epoxy liner to minimize the probability of lithium-concrete reaction and the absorption of tritium and other radioactive materials on the walls.
- Lithium-fire-retarding agents (*e.g.*, graphite powder) should be designed for effective lithium-fire control and located conveniently inside the confinement building.
- Drain tanks with a flame-retarding drain-pipe design are recommended. to reduce the impact of a lithium fire.
- The first wall and blanket must be drained to prevent a lithium fire when air is allowed into the confinement building.
- Because of the vanadium-alloy structural material of TITAN-I, a cool-down period of two to seven days will be needed for the afterheat to decay before draining the reactor torus. The exact waiting period will be determined by details of mechanical and passive heat-removal designs.

The impact of these guidelines and the safety design of the TITAN-I reactor are presented in the remaining part of this section.

### 13.3.2. Material Selection

One of the major concerns in the safety design is the post-shutdown afterheat induced in the structure because of the high neutron wall loading of the TITAN-I design

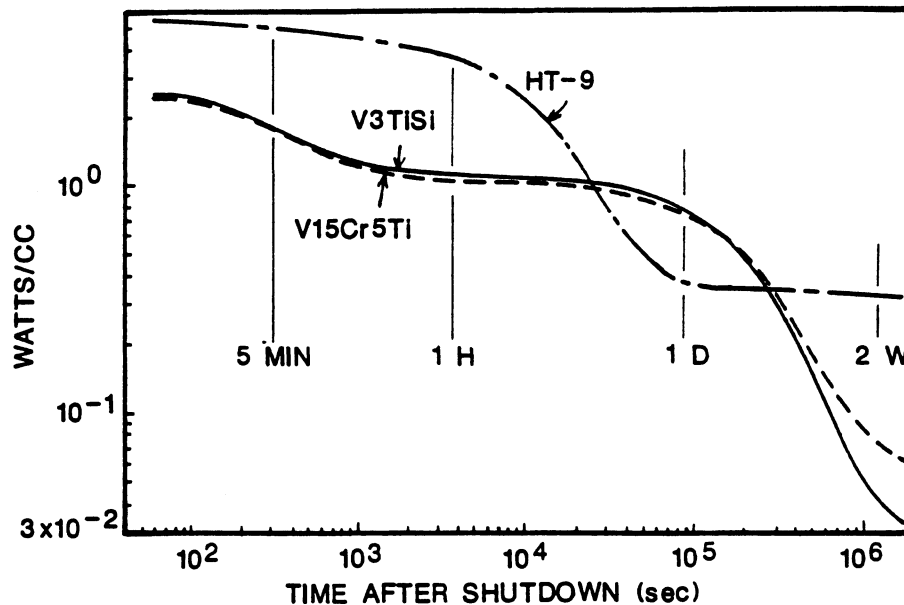


**Figure 13.3-1.** The first-wall afterheat for V-3Ti-1Si, V-15Cr-5Ti, and HT-9 as a function of time after shutdown for 1 FPY of operation at  $18 \text{ MW/m}^2$  of neutron wall loading.

( $18 \text{ MW/m}^2$ ). The afterheat levels at the first wall of TITAN-I were evaluated for three candidate structural alloys (V-3Ti-1Si, V-15Cr-5Ti, and HT-9). Figure 13.3-1 shows the afterheat power density at the first wall for these three alloys as a function of time after one full-power year (FPY) of operation at  $18 \text{ MW/m}^2$  of neutron wall loading. As shown, HT-9 has the highest level of afterheat among these three alloys for times to about six hours after shutdown, and for times after two days. The maximum power density in HT-9 is about  $5.5 \text{ W/cm}^3$  at shutdown. The afterheat is primarily from  $^{56}\text{Mn}$  (half-life of 2.6 h) which is induced in the major alloying element of the ferritic steel (iron) by the  $^{56}\text{Fe}(n,p)$  reaction. The  $^{56}\text{Mn}$  will decay away within one day, after which the afterheat is dominated by  $^{54}\text{Mn}$  (half-life of 313 d), a product of  $^{54}\text{Fe}(n,p)$  reaction.

The afterheat power densities for the two vanadium-based alloys are almost identical for about two days after shutdown, and are about a factor of two lower than HT-9 within the first hour after shutdown (Figure 13.3-1). The dominating radionuclides for the afterheat for both alloys are  $^{48}\text{Sc}$  (half-life of 43.7 h) produced by the  $^{51}\text{V}(n,\alpha)$  reaction,  $^{51}\text{Ti}$  (half-life of 5.76 min) by the  $^{51}\text{V}(n,p)$  reaction, and  $^{52}\text{V}$  (half-life of 3.75 min) by the  $^{51}\text{V}(n,\gamma)$  reaction, within about one week after shutdown.

For the first five minutes after shutdown, the silicon in V-3Ti-1Si contributes  $\sim 3\%$  of the total afterheat, primarily from  $^{28}\text{Al}$  (half-life of 2.24 min) produced by  $^{28}\text{Si}(n,p)$  reaction. After one week, the dominant radionuclide in V-3Ti-1Si is  $^{46}\text{Sc}$  (half-life of 83.8 d), a product of  $^{46}\text{Ti}(n,p)$  reaction. Because of a higher Ti content, the afterheat values (from  $^{46}\text{Sc}$ ) in V-15Cr-5Ti will be slightly higher than V-3Ti-1Si. In addition, V-15Cr-5Ti contains significant amounts of chromium and the decay heat from  $^{51}\text{Cr}$  (half-life of 27.7 d), produced by  $^{52}\text{Cr}(n,2n)$  and  $^{50}\text{Cr}(n,\gamma)$  reactions, should be considered.

These results indicate the significant advantage of the vanadium-base alloys in terms of lower afterheat power density within a few hours after shutdown and have influenced the selection of V-3Ti-1Si as the TITAN-I structural material.

### 13.3.3. Configuration and Lithium-Drain-Tank Design

The configuration of the TITAN-I FPC is illustrated in Figure 13.3-2, which shows the impact of the safety guidelines of Section 13.3.1. Three physical barriers (*i.e.*, blanket tubes, vacuum vessel, and confinement building) are used to separate the primary lithium from air and water. As illustrated, the primary-coolant connections are all located on top of the FPC to prevent complete drainage of the coolant. The worst accident for a lithium self-cooled design is perceived to be an uncontrolled lithium fire. To reduce the impact from this potential accident scenario, passive drain tanks were incorporated into the TITAN-I design.

Figure 13.3-3 shows the geometric model which was used in the design of the drain tanks and drain pipes in order to evaluate the feasibility of the proposed design approach. Two sets of drain tanks will be needed: one connected to the vacuum vessel and one to the confinement building. Also shown are passive fire-retarding valves to prevent fire propagation into the drain tanks. These valves will allow the heavier liquid lithium into the drain tanks and minimize the amount of air entering the system by closing the spring valve, as is illustrated in Figure 13.3-3. Based on the tank geometry and the drain-system dimensions (Figure 13.3-3), it was found that the complete lithium inventory can be drained in less than 30 seconds.

Design characteristics of the lithium-drain system are given in Table 13.3-I. The diameter of the drain pipes was selected to be 15 cm in order to avoid flow blockage caused by the high viscosity of the liquid lithium. Four and six drain tanks would be needed, respectively, for the vacuum vessel and confinement building zones; these tanks are sufficiently large to hold the potential lithium inventories from the primary and

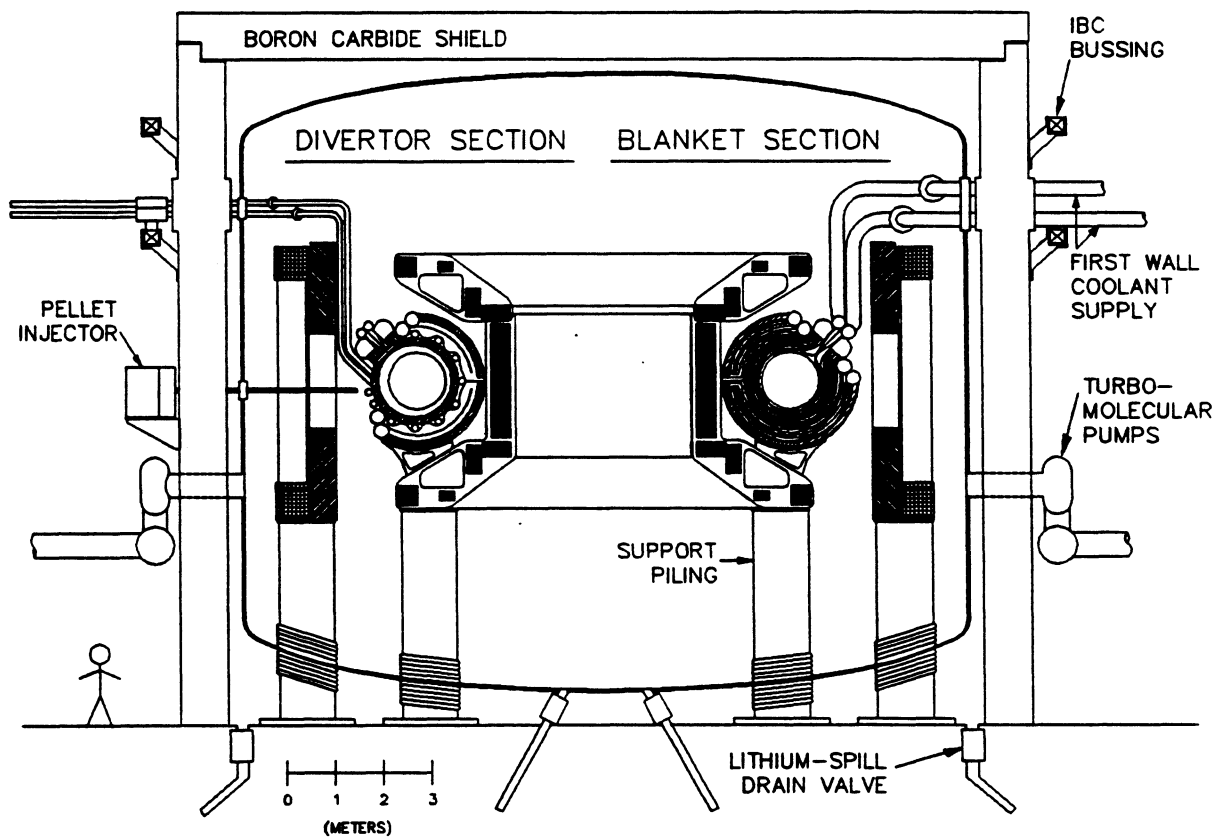


Figure 13.3-2. Elevation view of the TITAN-I fusion power core.

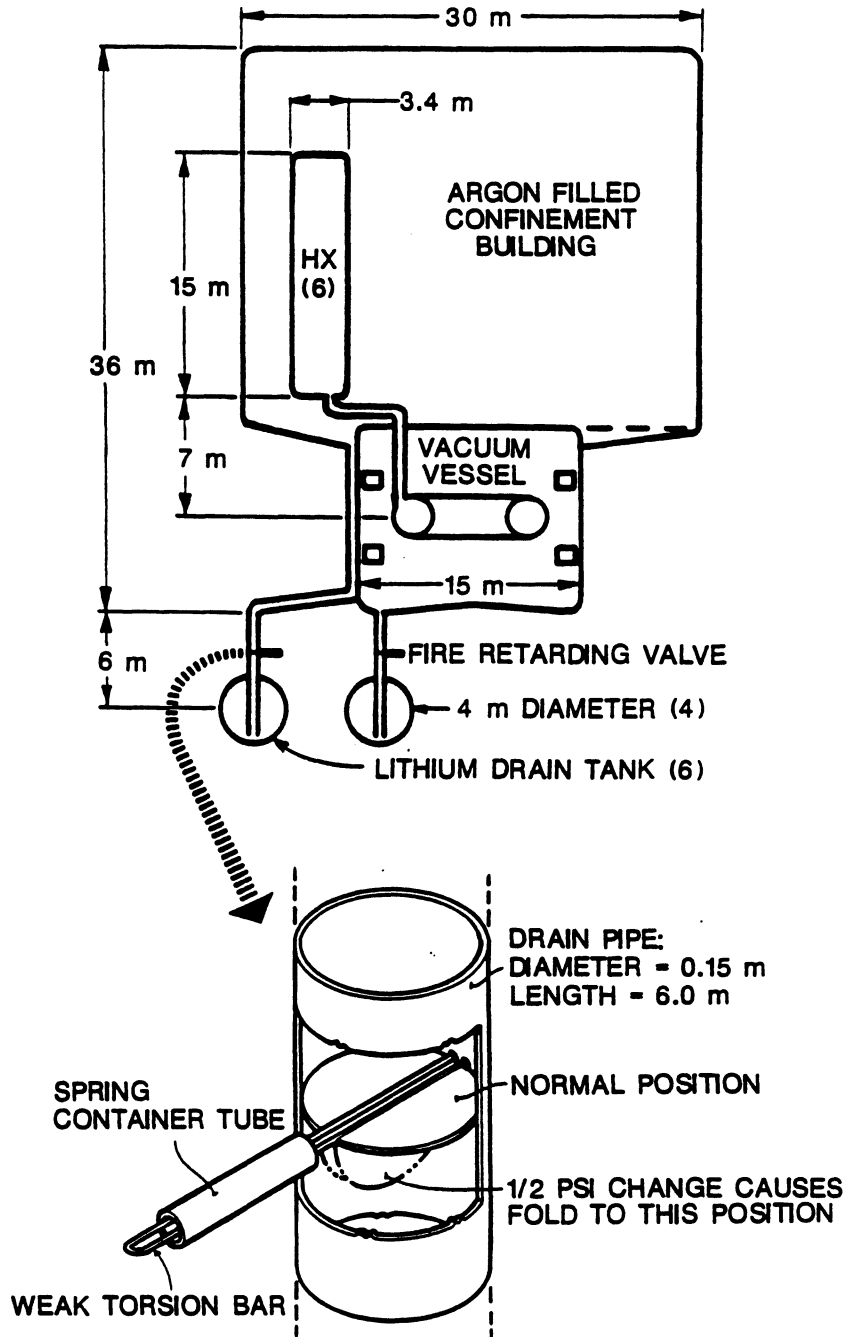


Figure 13.3-3. Elevation view of the TITAN-I reactor showing the geometry of the vacuum vessel, confinement building, drain tanks and pipes, and passive fire-retarding valves.

secondary loops. These cylindrical drain tanks are all 4 m in diameter and 9 m long and are spaced underneath the FPC such that they will not interfere with the structural supports of the FPC. The above observations indicate that the design of a fast lithium-drain system for TITAN-I is feasible.

#### 13.3.4. Confinement-Building Cover Gas

The vacuum vessel and all of the primary-coolant circuit of the TITAN-I design are enclosed in an inert cover gas. Different cover-gas options (helium, argon, and nitrogen) were evaluated and the results are summarized in Table 13.3-II.

Helium has the advantage of being chemically inert and will not produce radioactive isotopes. The disadvantages of helium are that it is relatively expensive and it is lighter than air so, unless it is contained, it will not function as a cover gas when it is mixed with air.

The most commonly used cover gas is nitrogen and it is the least expensive of the three. Nitrogen, however, reacts with lithium coolant and forms  $\text{Li}_3\text{N}$  which is a very corrosive compound. For investment protection under minor accident conditions, nitrogen would not be a suitable choice for the lithium self-cooled designs.

Argon is cheaper than helium and heavier than air, yet it has the key disadvantage of being activated by neutrons. The main argon activation-dose contributors are  $^{37}\text{S}$  (65%),  $^{40}\text{Cl}$  (14%), and  $^{41}\text{Ar}$  (12%). Smaller contributors are  $^{39}\text{Cl}$  and  $^{38}\text{Cl}$ . Neutron activation analysis and release-dose calculations were performed under accident and normal-release conditions for Ar, taking into consideration the TITAN-I configuration (Figure 13.3-2). It was found that the equilibrium concentrations of induced radioactivity in the argon cover gas were too high to satisfy the criteria for accidental and routine releases.

However, the amount of the induced radioactivity in the argon cover gas can be substantially reduced by additional shielding outside the vacuum vessel. For the TITAN-I design, a 1.2-m-thick concrete radiation shield was used. Dose-boundary calculations were performed for accidental release of the entire confinement building atmosphere (26,000  $\text{m}^3$  of argon) at ground level by a catastrophic building failure, assuming a short-term atmospheric-dilution factor of  $10^{-6} \text{ m}^{-3}$  at 1-km exclusion-area boundary (EAB) based on realistic site meteorological conditions. For these assumptions, the off-site dose is less than 5-mrem whole-body gamma dose, which is small compared to the 10CFR100 limit of 25 rem.

Table 13.3-I.

## CHARACTERISTICS OF THE TITAN-I LITHIUM-DRAIN SYSTEM

|                               | Vacuum Vessel | Confinement Building |
|-------------------------------|---------------|----------------------|
| <b>Lithium Coolant Loops:</b> |               |                      |
| $L$ (m)                       | 22.           | 22.                  |
| $d$ (m)                       | 0.5           | 0.5                  |
| $D$ (m)                       | 2.4           | 2.4                  |
| $V_0$ (m/s)                   | 20.8          | 20.8                 |
| Li mass (tonne)               | 212.          | 278.                 |
| No. of heat exchangers        | 6             | 6                    |
| Discharge time (s)            | 22.5          | 35.0                 |
| <b>Drain System:</b>          |               |                      |
| $L$ (m)                       | 6.            | 6.                   |
| $d$ (m)                       | 0.15          | 0.15                 |
| $D$ (m)                       | 15.           | 26.                  |
| $V_0$ (m/s)                   | 10.8          | 10.8                 |
| Li mass (tonne)               | 212.          | 278.                 |
| No. of drain pipes            | 100           | 90                   |
| Pipe separation (m)           | 0.47          | 1.0                  |
| Drain time (s)                | 22.2          | 32.3                 |
| <b>Drain Tank:</b>            |               |                      |
| Diameter (m)                  | 4.            | 4.                   |
| Length (m)                    | 9.            | 9.                   |
| No. of tanks                  | 4             | 6                    |

**Table 13.3-II.**  
**CONFINEMENT-BUILDING COVER GASES**

| Option   | Cost (1987 k\$) <sup>(a)</sup> | Comments   |
|----------|--------------------------------|--|
| Helium   | 69.0                           | <ul style="list-style-type: none"> <li>• Lighter than air</li> <li>• Relatively expensive</li> <li>• Nonreactive</li> </ul>  |
| Argon    | 27.5                           | <ul style="list-style-type: none"> <li>• Heavier than air<br/>(Major advantage under Li Fire)</li> <li>• Cheaper than He</li> </ul>                                    |
| Nitrogen | 2.8                            | <ul style="list-style-type: none"> <li>• Forms Li<sub>3</sub>N</li> <li>• Cheapest</li> <li>• Li-N reaction (<math>T_{max} \sim 830^{\circ}\text{C}</math>)</li> </ul> |

(a) Cost for confinement building volume of 26,000 m<sup>3</sup>.

For normal operating conditions, the off-site dose is determined by the activity concentrations in the confinement building and the volumetric leakage rate. Assuming a volumetric leakage rate of 1% per day, and a typical average atmospheric dilution at 1 km of  $7.6 \times 10^{-7} \text{ m}^3$ , the annual whole-body gamma dose can be kept below the 5-rem limit of 10CFR50. Based on these observations and the key advantage of being heavier than air, argon was selected as the confinement-building cover gas for the TITAN-I design.

### 13.3.5. Tritium Issues

Other safety results from this study concern tritium. At a tritium concentration of 1 appm, the total tritium inventories in the primary coolant loop is 275 g and a similar.

amount is in the secondary loop. Since passive drain tanks are used to drain a large fraction of the tritiated lithium, under the worst accidental conditions the amount of possible tritium release will be  $< 200$  g. The tritium inventory in the blanket structure was estimated to be  $< 10$  g, which is acceptable. The tritium leakage rate from the primary loop was estimated to be 7 Ci/d, which is within the 10 Ci/d limit [9].

#### 13.4. LOSS-OF-FLOW & LOSS-OF-COOLANT ACCIDENTS

Two of the major accidents postulated for the FPC are the loss-of-flow accident (LOFA) and the loss-of-coolant accident (LOCA). Demonstration of the level of safety attainable by the power plant requires in-depth analyses of the response of the FPC to these accidents. Thermal responses of the first wall, blanket, and shield of the TITAN-I design to LOFA and LOCA are modeled using a finite-element heat-conduction code. The results of these analyses helped guide the engineering design of the reactor so that the maximum level of safety can be achieved.

The principal concern of these analyses is to estimate the temperature history and peak temperature of the FPC during the accident and to predict the behavior of the structural material at these temperatures. Several temperature limits have been identified for the V-3Ti-1Si alloy and are summarized in Table 13.4-I. The first important limit ( $\sim 1300^\circ\text{C}$ ) corresponds to the onset of volatilization of radioactive products (CaO, SrO) in the vanadium alloy. Although not an immediate safety hazard, simultaneous breach of the vacuum tank and the confinement building would release these products into the biosphere. A more stringent temperature limit is the recrystallization temperature of the vanadium alloy ( $\sim 1100^\circ\text{C}$ ). If the temperature of the structure exceeds this value, then the strength of the material is severely degraded and the torus assembly must be replaced. Details of the recrystallization phenomenon are found in Section 10.2. For the TITAN-I design, the worst-case accident scenario should not result in peak temperatures in excess of  $1100^\circ\text{C}$ .

In addition to the above temperature limits, the impact of the thermal transient on the structural material should be considered. During such thermal transients, creep rupture is the dominant mechanism of structural failure. The time-to-failure of the creeping structural material of the FPC should be sufficiently long to ensure that structural integrity of the FPC is maintained and that a small-scale accident would not lead to more serious accident (Section 13.4.3).

**Table 13.4-I.**  
**TEMPERATURE LIMITS FOR TITAN-I FPC<sup>(a)</sup>**

---

|  |           |
|--|-----------|
| Melting point of the vanadium alloy                  | 1890 °C   |
| Onset of activation product release                  | ~ 1300 °C |
| Recrystallization of the vanadium alloy              | ~ 1100 °C |
| Maximum vanadium temperature during normal operation | 750 °C    |
| Boiling point of lithium                             | 1347 °C   |
| Solidification temperature of lithium                | 181 °C    |

---

(a) Time-to-failure by thermal creep rupture is decreased at elevated temperatures.

#### 13.4.1. Accident Models

An elevation view of TITAN-I is shown in Figure 13.4-1. A mid-plane cross section of the first wall, integrated blanket coil (IBC), and hot shield (Figure 13.4-2) shows the repetitive nature of the toroidal and radial cross sections. Therefore, a 2-D geometric model can be used to represent the radial build of the blanket, as is shown in Figure 13.4-3. The coarseness of this finite-element mesh may first appear to be inconsistent with transient-problem analysis. The problem under study, however, is primarily one of heat capacity and heat flow between components which is mainly governed by the radiation between surfaces and, therefore, should be insensitive to the size of the computational elements within the materials.

An alternate 2-D model of the blanket would provide a poloidal/radial build similar to Figure 13.4-1. This model would incorporate the heat conduction along the poloidal flow paths but would not accurately account for the tube-to-tube radiation seen in Figures 13.4-2 and 13.4-3. Since the poloidal conduction path along the first-wall tubes is long (2.09 m) and the initial temperatures are relatively high (700 °C), the radial heat flow during accidents is dominated by thermal radiation.

In order to determine the maximum temperature in the system, the initial and boundary conditions and spatial and temporal distribution of loads are needed. The applied

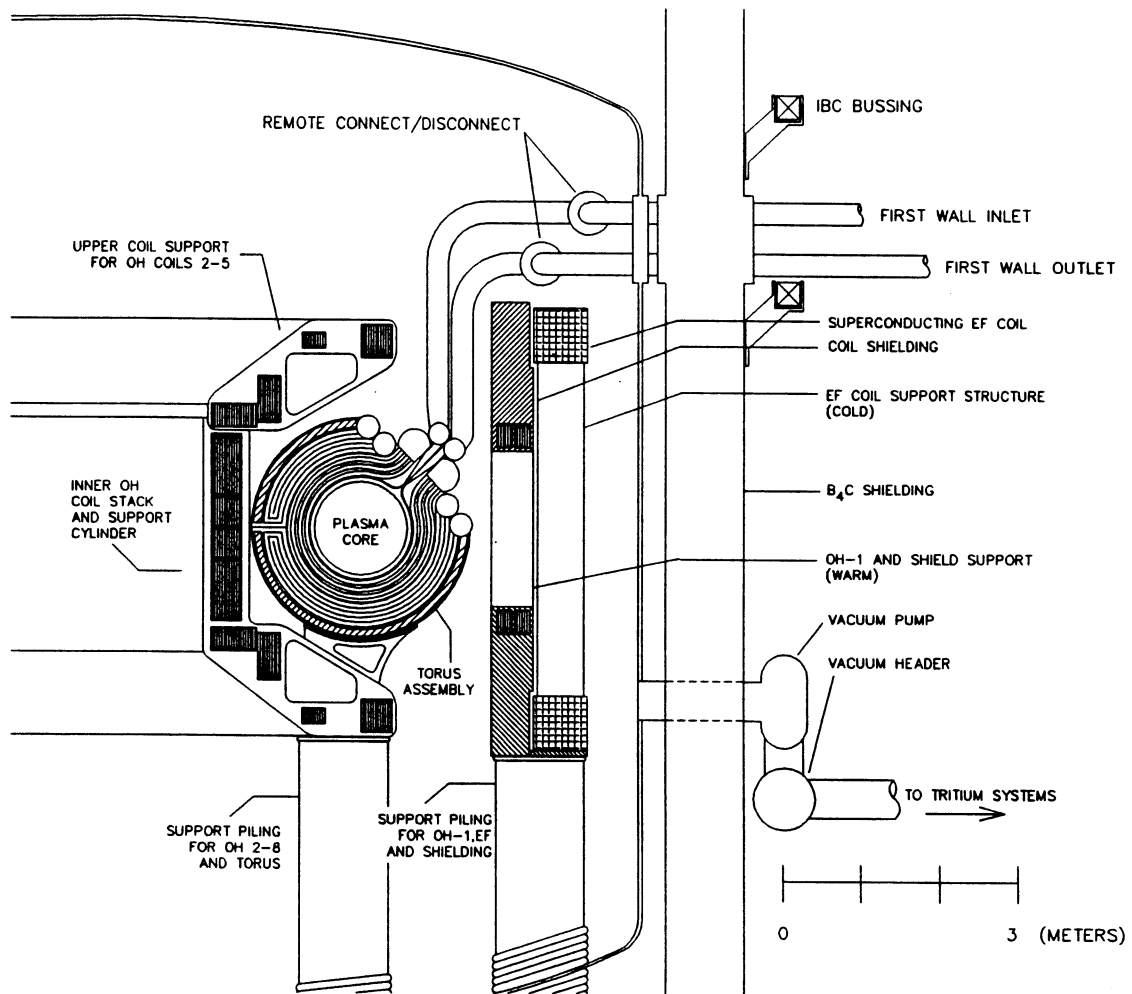


Figure 13.4-1. An elevation view of the TITAN-I fusion power core.

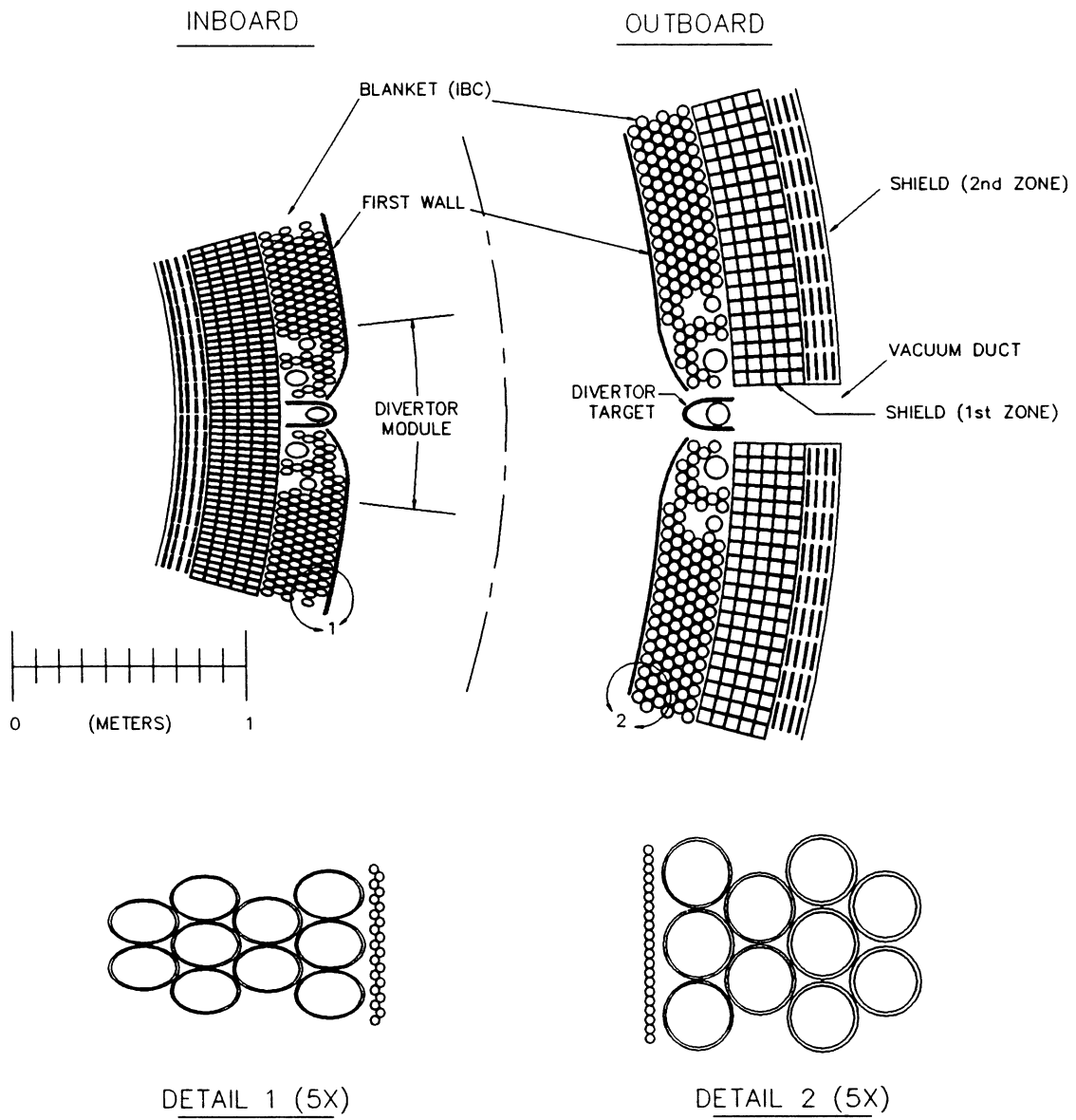
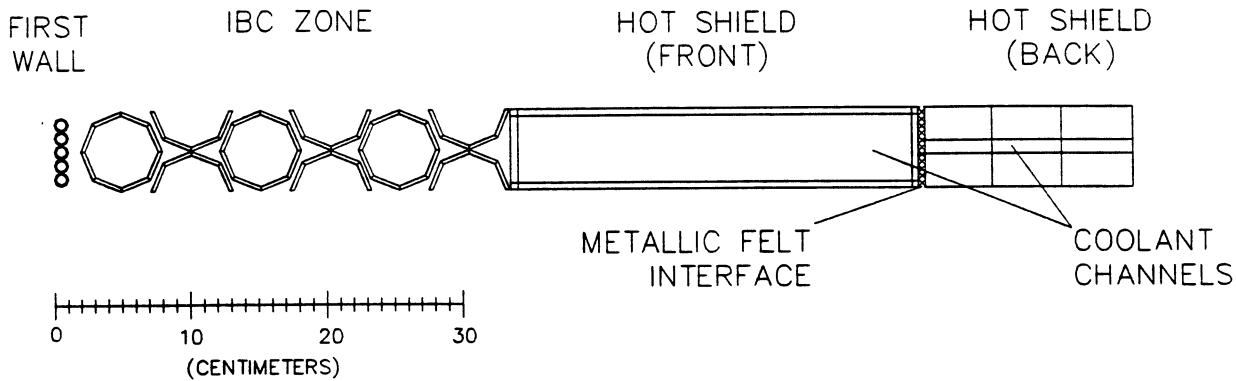


Figure 13.4-2. Mid-plane cross section of the TITAN-I fusion power core.



**Figure 13.4-3.** Finite-element model of the TITAN-I fusion power core used in LOFA and LOCA analyses.

boundary conditions include radiation to a constant-temperature sink (behind the shield), as well as internal radiation between various surfaces in the FPC. In LOFA analyses, internal radiation conditions are only applied to the outer surfaces of the tubes, while in the LOCA model, radiation conditions are applied to the internal cavities of the piping as well as to the outer surfaces. Table 13.4-II lists the emissivities and radiation view factors for various locations in the blanket. The view factors are calculated numerically by the code.

The initial temperature of the blanket differs for the LOCA and LOFA. Following the initiation of a LOFA, pump coast down will take place. During the coast-down period, which could last several minutes if the pump has enough inertia, the primary coolant continues to circulate while the plasma is shut down. The continued circulation is assumed to allow the first-wall and blanket streams to mix and equilibrate thermally. Therefore, at the onset of the LOFA analysis, the blanket-coolant temperature is set equal to the mixed bulk temperature of the lithium.

The initial temperature of the blanket for the LOCA analysis depends on several assumptions about the accident scenario. Because of the finite drain time required to empty the primary loop following a pipe break, an instantaneous loss of coolant is unlikely. However, an instantaneous plasma shutdown at the instant of a pipe break is also unlikely. Relatively rapid plasma-shutdown mechanisms have been proposed (Sections 6 and 13.6).

Typical plasma-shutdown times are on the order of a second while the primary-loop drain time is less than 30 s. The longer duration of the coolant drain will allow the removal of heat added by the plasma prior to its shutdown. The temperature of the blanket at the end of the coolant drain period is conservatively set equal to the full-power operating conditions. In reality, coolant draining that continues after the termination of

**Table 13.4-II.**  
**EMISSIVITY AND VIEW FACTORS OF TITAN-I FPC**

| Participating Surfaces                                | Emissivity | View Factor <sup>(a)</sup> |
|---|------------|----------------------------|
| First-wall tubes to first row of IBC                  | 0.50       | 0.70                       |
| Inside of IBC tubes: front half to back               | 0.25       | 0.67                       |
| Outside of IBC tubes: between adjacent rows           | 0.50       | 0.75                       |
| Last IBC tube to hot shield                           | 0.50       | 0.75                       |
| Inside of hot-shield coolant channels (zone 1)        |            |                            |
| Front to back   | 0.25       | 0.15                       |
| Front to one side                                     | 0.25       | 0.43                       |
| Zone 1 of hot shield to zone 2 <sup>(b)</sup>         | N/A        | N/A                        |
| Inside of hot-shield coolant channels (zone 2)        |            |                            |
| Front to back   | 0.25       | 0.20                       |
| Front to one side                                     | 0.25       | 0.40                       |
| Back of hot shield to sink (OH coils and vacuum tank) | 0.50       | 1.00                       |

(a) Tabulated view factors are based on the average of the view factors for the individual finite-element surfaces associated with the participating surfaces.

(b) The interface between the two zones of the hot shield is a 1-cm metallic felt to provide support for the torus. It is thus treated as a part of the thermal-conduction solution.

the plasma will continue to cool the structure. A more realistic initial LOCA temperature is somewhere between the full-power operating conditions and the bulk temperature of the coolant. Uncertainties in the exact dynamics of the LOCA initiation suggest the use of the conservative initial temperatures (full-power conditions).

The spatial variation of the afterheat at shutdown is shown in Figure 13.4-4. The time dependence of the decay heat in the first wall is shown in Figure 13.4-5. The exclusive use of V-3Ti-1Si throughout the torus produces low levels of decay afterheat. The initial heating rate in the first wall of  $2.1 \text{ W/cm}^3$  drops rapidly to less than  $1 \text{ W/cm}^3$  in about three hours. The static lithium of the LOFA analysis has no internal heat generation and acts as a heat sink.

Several heat conduction codes are available to model the thermal response of the system during LOCA and LOFA scenarios described above. Finite-element codes such as ANSYS [10], TACO2D [11], and TOPAZ [12] have sufficient flexibility to solve this time-dependant, nonlinear problem. For the safety analysis of the TITAN-I design, TACO2D is used and analytical checks are provided, when possible, to verify the results.

#### 13.4.2. Thermal Response to LOCA and LOFA

The first case studied is that of a complete LOCA. If the results from this case indicate that the blanket will survive a LOCA, then the blanket should also survive a LOFA. The thermal response of the first wall, IBC, and shield are shown in Figure 13.4-6. The peak temperature attained is  $1500^\circ\text{C}$  indicating that the TITAN-I blanket will not melt during a LOCA (Table 13.4-I). The temperature, however, exceeds the recrystallization temperature of the vanadium alloy ( $\sim 1100^\circ\text{C}$ ). Although exceeding this temperature does not pose a direct safety hazard, it does require that the torus assembly be replaced subsequent to the accident. The peak temperature of  $1500^\circ\text{C}$ , also exceeds the temperature limit of  $1300^\circ\text{C}$  for the onset of the volatilization and release of the radioactive products in the vanadium alloy such as CaO and SrO (Table 13.4-I). These products will become mobile within the vacuum tank and, although not an immediate safety hazard, simultaneous breach of the vacuum tank and the containment building will release these products to the biosphere.

The above results do not include the effects of a lithium fire during the LOCA. The lithium-fire calculations are discussed in detail in Section 13.5 and the results then incorporated in the form of prescribed temperature histories during the lithium-burn period. The primary effect of the lithium fire is an increase in the temperature of the

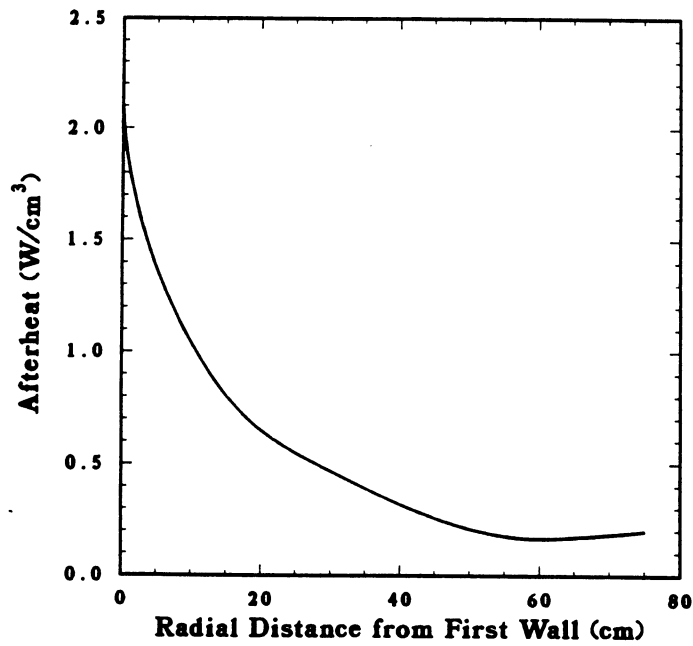


Figure 13.4-4. The level of decay afterheat in the TITAN-I FPC at shutdown.

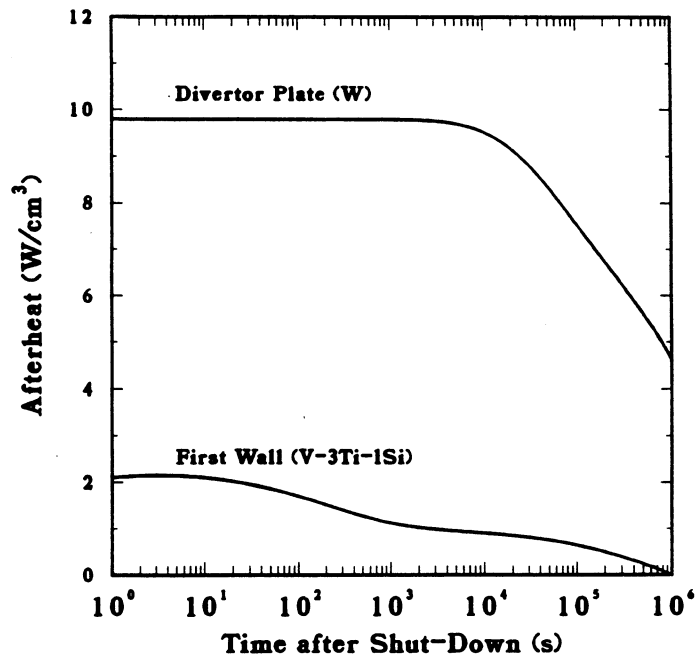
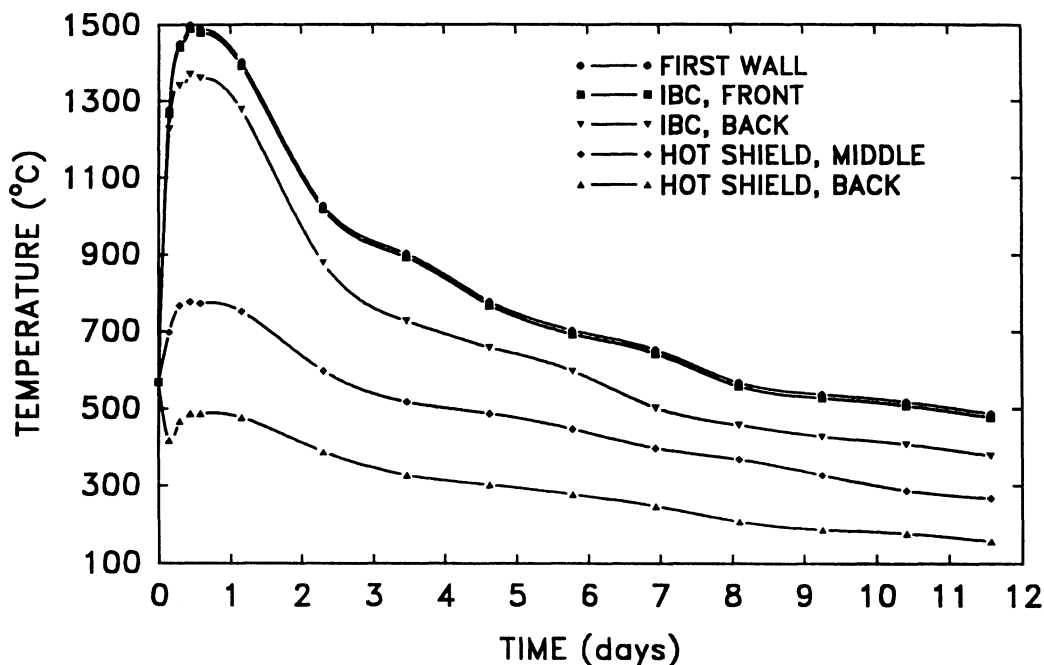


Figure 13.4-5. The level of decay afterheat in the TITAN-I first wall and divertor plate as a function of time after shutdown.



**Figure 13.4-6.** The thermal response of the TITAN-I FPC to a complete LOCA as a function of time after the initiation of the accident.

vacuum tank and inner ohmic-heating coils, both of which are the ultimate heat sink for the thermal radiation from the torus assembly. Because of the short duration of the lithium fire ( $\sim 30$  s), the corresponding temperature rise in the surrounding structures is small ( $5^\circ\text{C}$ ). The effect of the fire on the first-wall peak temperature is minimal. The first wall is well separated from the back of the torus where the fire is burning, and, therefore, it is fairly insensitive to short-duration events such as the 30-s fire. For these short-duration events, the first wall can be treated as a simple heat-capacity problem, sensitive only to events occurring in the immediate vicinity.

The temperature histories during a LOFA are plotted in Figure 13.4-7. The peak temperature is  $990^\circ\text{C}$  and occurs at the first wall, 12.8 hours after accident initiation. This peak temperature satisfies all of the constraints listed in Table 13.4-I. The heat capacity of the static lithium accounts for the moderate temperature excursion. The heat capacity of the lithium in the primary loop, away from the blanket, was not included. No natural convection of the coolant is assumed in the analysis even though the emergency plasma shutdown procedure of Section 13.6 is accompanied by the discharge of all magnets and no MHD retarding force is expected on the coolant. If natural convection develops, the temperature excursions will be considerably smaller than those predicted by Figure 13.4-7.

Material and configuration differences between the divertor and the blanket necessitate additional LOFA analysis for the divertor region. The high initial level of decay afterheat and its longevity relative to the vanadium are a concern. Although the tungsten neutralizer plate is capable of high-temperature operation, the attached vanadium cooling tubes are subject to the same limits as the first wall and blanket. Excessive heating in the divertor structure has the potential to create vanadium-tube failures, hence a local LOCA.

The finite-element mesh used to model the divertor region is shown in Figure 13.4-8. The initial level of afterheat in the tungsten alloy is  $10 \text{ W/cm}^3$  and remains relatively constant for  $10^4 \text{ s}$ . The solid angle for thermal radiation from the divertor plate, across the plasma chamber, and onto the opposite side of the divertor is small; hence, the view factor is set to 1.0, and the temperature boundary condition of the sink is the time-varying first-wall temperature, as is calculated by the first-wall and blanket LOFA analysis. The heating rates in the vanadium structure are the same as those in the first-wall and blanket analysis.

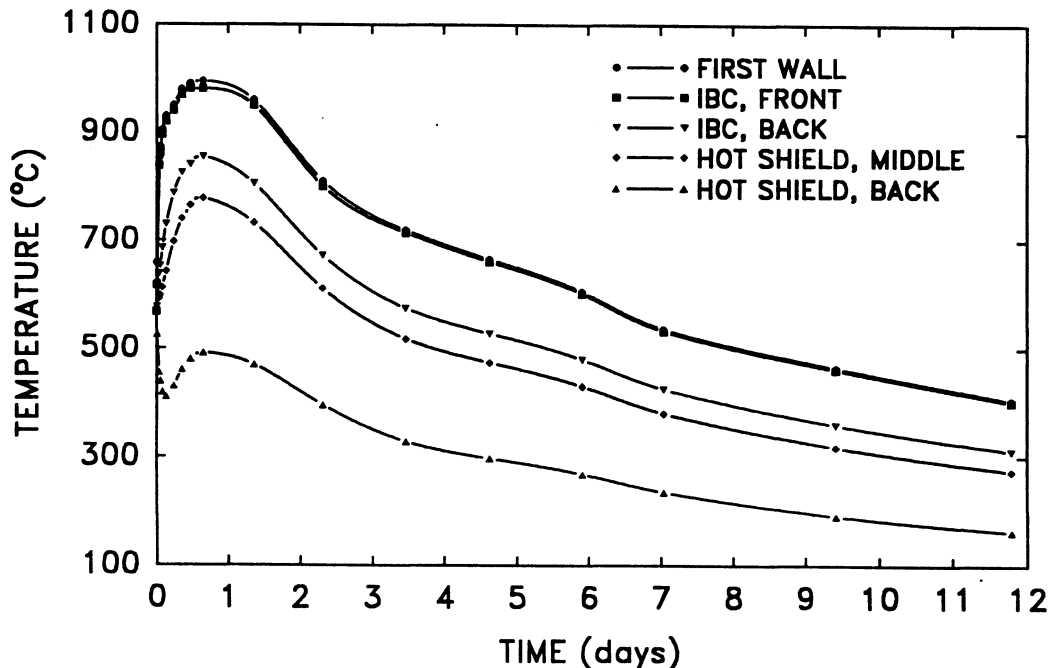


Figure 13.4-7. The thermal response of the TITAN-I FPC to a complete LOFA as a function of time after the initiation of the accident.

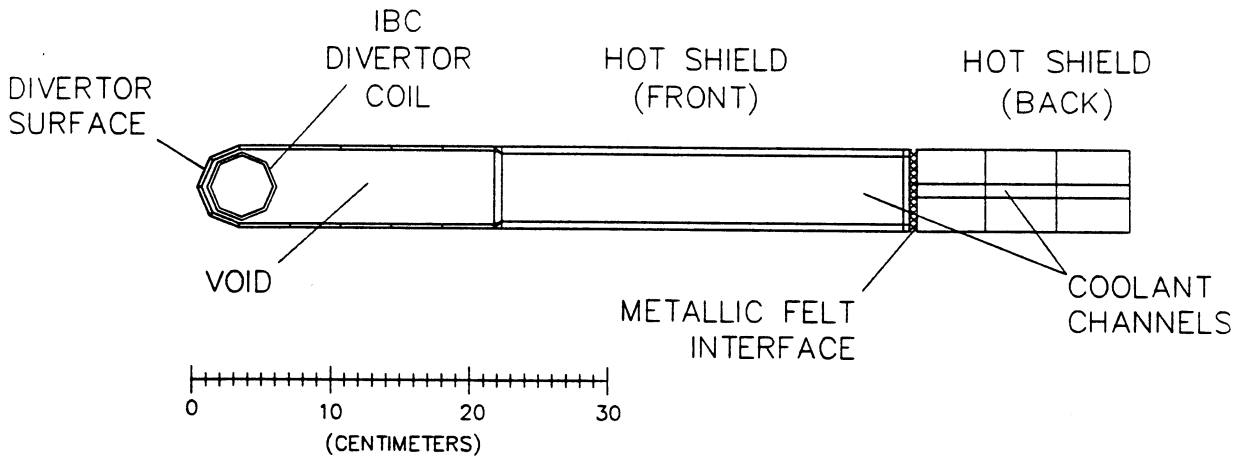


Figure 13.4-8. Finite-element model of the TITAN-I fusion power core used in divertor LOFA analysis.

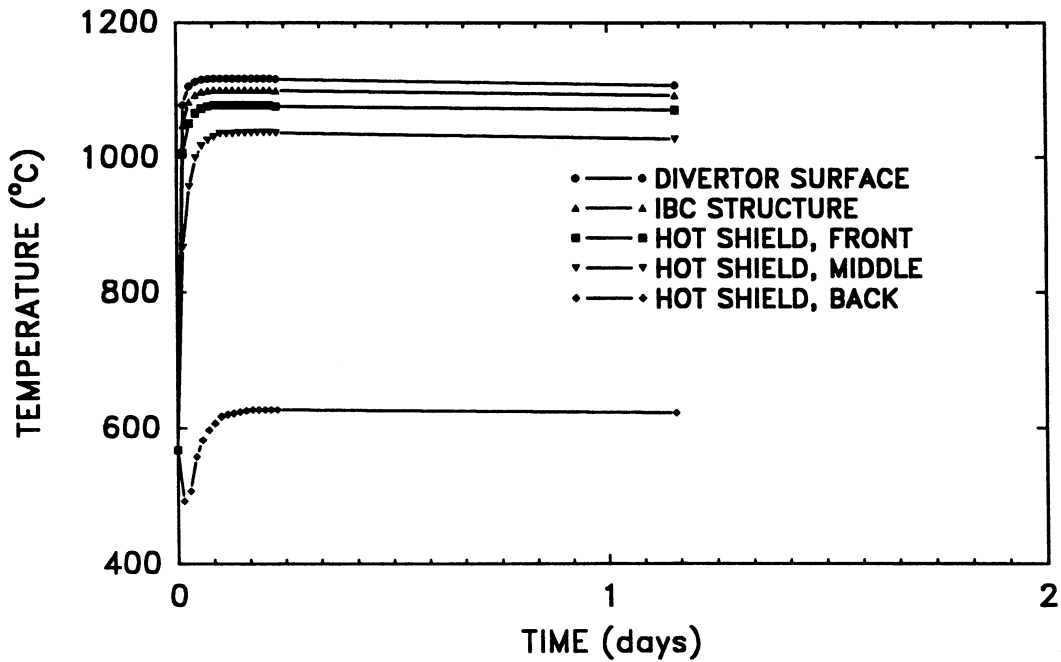


Figure 13.4-9. The thermal response of the TITAN-I FPC to a complete divertor LOFA as a function of time after the initiation of the accident.

The temperature histories of the divertor tungsten armor, divertor-IBC structure, and divertor shield is plotted in Figure 13.4-9. The peak temperature in the vanadium is 1117°C and occurs in the cooling tube behind the front of the divertor plate. The peak temperature is slightly higher than the recrystallization temperature of V-3Ti-1Si (~ 1100°C). Even though the failure of the divertor is unlikely, the strength of the vanadium will be reduced significantly and the divertor module may not be able to operate at full-power conditions after LOFA.

In the TITAN-I design, all of the primary-coolant routings and connections are above the FPC. In case of a major pipe break outside the FPC, the coolant remains in the reactor torus. Even if several coolant tubes inside the FPC (at the lowest point) rupture, the drain time for the coolant would be very long because of the large lithium inventory in the primary loop. Therefore, the possibility of a credible complete LOCA is eliminated. The worst local LOCA scenario envisioned for the TITAN-I design is a complete LOCA in the first-wall circuit and a LOFA in the blanket circuit. The thermal response of the FPC is found to be similar to that of a complete LOFA. Therefore, partial LOCA in the TITAN-I design will not result in any safety concerns.

### 13.4.3. Elevated-Temperature Creep Rupture

During a LOFA, lithium remains inside the torus assembly and, because of the static head of lithium in the primary loop, a hydrostatic pressure load exists inside the piping (typically 0.1 to 0.2 MPa). The hydrostatic pressure and the elevated temperature of the blanket could lead to failures through thermal-creep rupture. Should this occur, a LOCA situation would develop. An estimate of the time to rupture of the TITAN-I first wall and blanket during a LOFA is provided here.

For a component of a given material, the time to rupture depends on the temperature and stress. The failure analysis of creeping structural materials is made difficult by data shortages for specific materials (*e.g.*, accounting for impurities and heat treatments) in specific stress and temperature ranges, and the process is further complicated by the difficulty of the inelastic stress analysis. Because of the complexity of creep deformation, designers rely heavily on empirical equations to predict creep deformation. For vanadium-base alloys, the expected service life is much longer than the duration for which experimental creep data are available. Extrapolation of the creep data, in particular the creep-rupture data, to longer times have been studied extensively over the past decades [13 - 15].

Widely used extrapolation techniques for creep-rupture data include the Larson-Miller, White-LeMay, and Orr-Sherby-Dorn methods [13]. These methods predict the value of the rupture time,  $t_r$ , as a function of the material temperature and for different applied stresses. The choice and success of these methods depends on the behavior of the creep-rupture data and assumed pattern for the data in each method. As a result, it is possible for these methods to predict different values of stresses appropriate to long-life conditions [13]. To overcome this problem, the minimum-commitment method (MCM) was developed at NASA [14] to extrapolate creep-rupture data without forcing the creep data set to any specific pattern. Ghoniem *et al.* [15] developed a modified-minimum-commitment method (MMCM) in which the stress, the time to rupture, and the temperature are related by the following functional form:

$$\ln(\sigma_r) = A(T) + B(T) \ln(t_r), \quad (13.4-1)$$

where  $\sigma_r$  is the stress to rupture in MPa,  $t_r$  is the time to rupture in hours, and  $A(T)$  and  $B(T)$  are temperature-dependent parameters given by

$$A(T) = a_o + a_1 T \quad \text{and} \quad B(T) = b_o + b_1 T. \quad (13.4-2)$$

Here,  $T$  is the temperature (K) and  $a_o, a_1, b_o,$  and  $b_1$  are constants determined by fitting creep-rupture data. The coefficients of Equation 13.4-2 for V-3Ti-1Si and V-15Cr-5Ti are given in Table 13.4-III.

Creep-rupture stress data for vanadium alloys, in particular for V-3Ti-1Si, are limited. Some V-3Ti-1Si creep-rupture stress data [16] are available at 750 and 850 °C. At 650 °C data were found only for a V-3Ti alloy containing unspecified amounts of silicon. The creep-rupture data at these three temperatures are used to develop a phenomenological stress-rupture equation (similar to Equation 13.4-1). A similar equation was also developed for V-15Cr-5Ti using more recent creep-rupture data [17].

Figure 13.4-10 shows the experimental data points [16] and estimates from MMCM for the creep-rupture stress of V-3Ti-1Si at several temperatures as well as the expected stress range in the first wall of TITAN-I during normal and off-normal operation. Based on the results of the MMCM extrapolation equation, operation of the first wall at a pressure close to 100 MPa and at temperatures below 700 °C will not lead to creep rupture within one year of normal operation. During off-normal conditions, coolant pressure is lost and creep rupture would not occur even if the structure is kept at elevated temperatures (1000 °C) for a prolonged period of time. However, high-temperature (> 850 °C) creep-rupture data are necessary to gain more confidence in the creep-rupture behavior at these

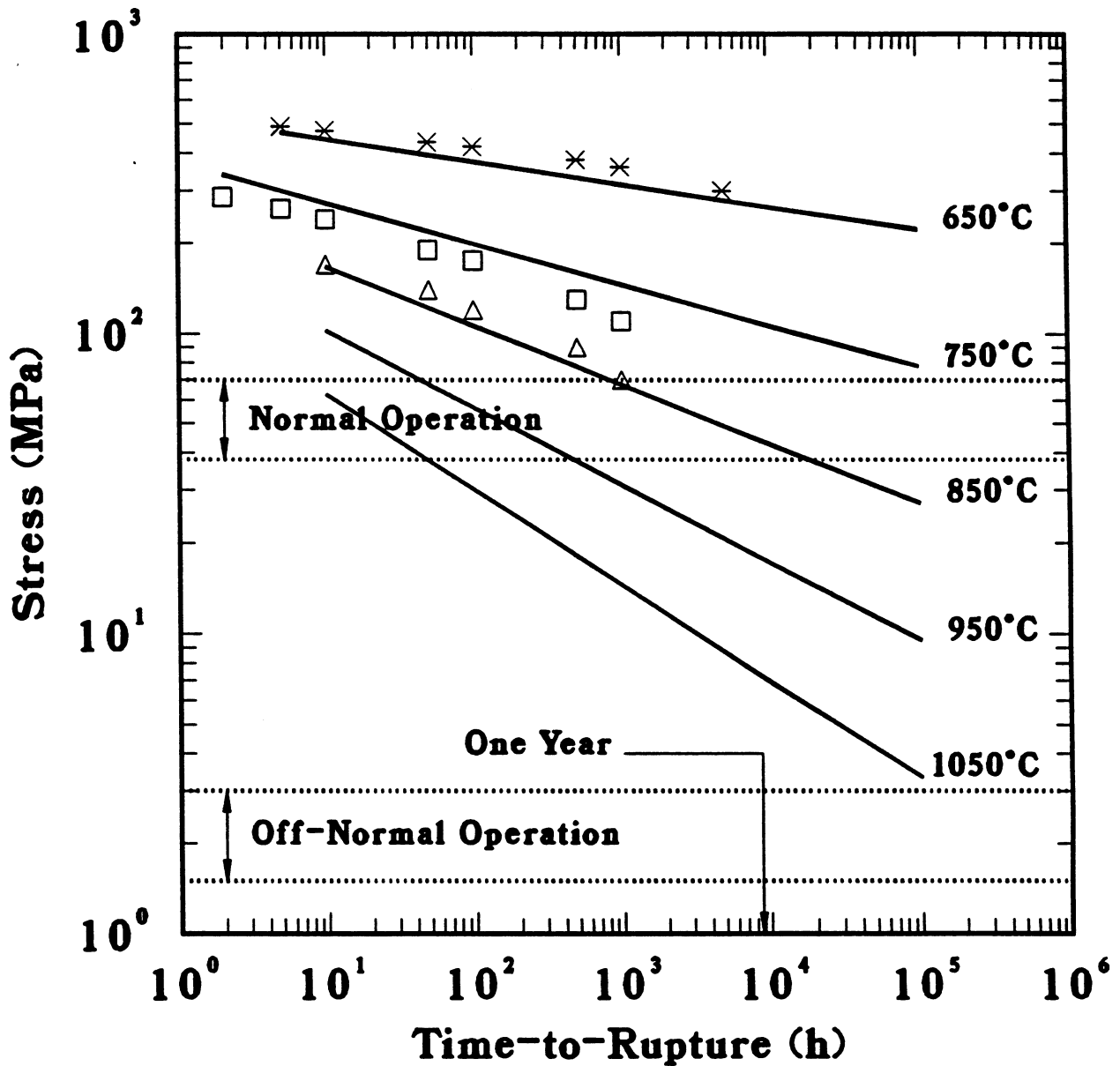


Figure 13.4-10. Creep-rupture stresses of V-3Ti-1Si at various temperatures. Symbols are data [16] and solid lines are estimated by MMCM. The expected stress ranges during normal and off-normal operations of the TITAN-I design are also shown.

**Table 13.4-III.**  
**COEFFICIENTS FOR THE CREEP-RUPTURE STRESS EQUATION**

| Coefficient | V-3Ti-1Si                 | V-15Cr-5Ti                |
|-------------|---------------------------|---------------------------|
| $a_o$       | 9.507209                  | 7.239522                  |
| $a_1$       | $-3.50498 \times 10^{-3}$ | $-1.04844 \times 10^{-3}$ |
| $b_o$       | $4.85748 \times 10^{-1}$  | $2.17853 \times 10^{-2}$  |
| $b_1$       | $-6.07858 \times 10^{-4}$ | $-7.38258 \times 10^{-5}$ |

higher temperatures. A more detailed discussion of the creep behavior of the vanadium alloys is given in Section 10.2.

The life-fraction rule (LFR) [18] is used to determine creep-rupture times under transient stress conditions. Several examples of the use of LFR method are given in Reference [19]. The LFR divides the component life into small time steps,  $dt$ , and assumes that the fraction of damage incurred by the material during any increment is determined by the ratio of the length of the time step to the rupture time,  $t_r$ , measured for the instantaneous temperature and stress during that time step,  $dt/t_r$ . When the accumulated damage fraction reaches unity, failure is assumed to occur. This rule, of course, assumes that the damage incurred during a time step is independent of the previously accumulated damage. The integral form of the LFR can be stated as follows:

$$\int_0^{t_f} \frac{dt}{t_r} = 1, \quad (13.4-3)$$

where  $t_f$  is the failure time for a transient-stress situation. To compute the failure time, Equation 13.4-1 is solved for the rupture time as a function of temperature and stress and substituted into the integral in Equation 13.4-3. Then, for a given stress history, the failure time,  $t_f$ , can be determined.

During normal operation, the thermal gradient in the first wall creates thermal stresses, while the primary stress results from the coolant pressure. After only a few displacements per atom (dpa), irradiation creep will relax the thermal component of the

stress and only the primary stress of the pressure will remain. During a LOFA, the primary stress is significantly reduced because the coolant pressure is lost. On the other hand, the thermal gradient is removed and a residual stress of opposite sign to the initial thermal stresses will develop. Hence, the stress field during a LOFA consists of a small primary stress, caused by the hydrostatic pressure load inside the piping, and an initial thermal stress of the same order as the operating thermal stress. If the LOFA occurs before the operating thermal stresses are completely relaxed, the stresses during the accident will be lower and failure will occur later.

During the thermal transient of an accident, the stress fields in both the first wall and blanket feature a maximum stress of the form

$$\sigma = \sigma_p + f(\sigma_o, t), \quad (13.4-4)$$

where  $\sigma_p$  is the primary stress and  $f(\sigma_o, t)$  is a decay function representing the time dependence of the initial thermal stress,  $\sigma_o$ . In the TITAN-I first wall, the pressure stress is about 1 to 2 MPa during LOFA and the initial thermal stress is about 200 MPa. In the blanket, the pressure stresses are of the same order, the thermal stresses are much smaller, and the temperatures are lower; the blanket, therefore, is expected to have a longer lifetime than after the first wall.

The decay function,  $f(\sigma_o, t)$ , depends on the creep-rate equation exhibited by a particular material. Typically, creep-rate equations are given in the form

$$\dot{\epsilon}_c = C \sigma^n, \quad (13.4-5)$$

where  $\dot{\epsilon}_c$  is the creep rate,  $C$  is a constant, and  $n$  is the creep exponent (both  $C$  and  $n$  are temperature dependent). When  $n = 1$ , the creep rate is proportional to the stress,  $\sigma$ , and the decay function is given by:

$$f(\sigma_o, t) = \sigma_o e^{-E C t}, \quad (13.4-6)$$

while for  $n > 1$ ,

$$f(\sigma_o, t) = \left[ \sigma_o^{1-n} - (1-n) E C t \right]^{1/(1-n)}, \quad (13.4-7)$$

where  $\sigma_o$  is the initial stress and  $E$  is the modulus of elasticity. For V-Ti alloys, the creep exponent,  $n$ , drops below 2 above  $\sim 800^\circ\text{C}$  [16], so a reasonable approximation would be to use Equation 13.4-6 for the decay function. Substituting Equation 13.4-6 in Equation 13.4-4, and applying the resultant stress history to Equation 13.4-1 will result

in the rupture time,  $t_r$ , as a function of the instantaneous temperature and stress. Then, Equation 13.4-3 can be used to find the time to failure,  $t_f$ .

For pure thermal stresses ( $\sigma_p = 0$ ), the stress,  $\sigma$ , decays exponentially from the initial thermal stress and the time to failure would be:

$$t_f = \frac{B}{EC} \ln \left[ 1 + \frac{EC}{B} \left( \frac{\sigma_o}{e^A} \right)^{1/B} \right], \quad (13.4-8)$$

where  $A$  and  $B$  are given by Equation 13.4-2. Because  $B$  is negative in the temperature range of interest, the right-hand side of Equation 13.4-8 is positive only if

$$C < -\frac{B}{E} \left( \frac{e^A}{\sigma_o} \right)^{1/B}, \quad (13.4-9)$$

which implies that rupture will not occur if the creep rate is sufficiently high to relax the stress before rupture occurs. For the TITAN-I first wall, pure thermal stresses will not cause failure at the expected LOFA temperature of  $\sim 1000^\circ\text{C}$  if the creep coefficient  $C$  is greater than  $10^{-5}/\text{h-MPa}$ . Since the creep rate of V-Ti alloys at  $1000^\circ\text{C}$  is, conservatively, 1%/h at stresses above 100 MPa [16], the creep coefficient of these alloys at  $1000^\circ\text{C}$  should be greater than 0.005/h-MPa, much larger than the limiting value from Equation 13.4-9. Therefore, the TITAN-I first wall would not fail under pure thermal stresses. This result is apparent if one considers the creep strain which develops during total relaxation of a 200-MPa thermal stress, as compared to the rupture strain at  $1000^\circ\text{C}$ . For unirradiated V-Ti alloys with Ti contents of 3% to 5%, the creep-rupture strain is well above 10% [16], whereas the total creep strain caused by relaxation of a 200-MPa thermal stress is only 0.17%. Therefore, the creep ductility is well above the strain produced and failure will not occur unless significant primary stresses are also present.

Because primary stresses are not relaxed by creep, they are much more likely to cause creep rupture. Considering creep rupture caused by only the primary stresses (the stress and temperature are constant in time), Equation 13.4-1 can be used for rupture time directly. The predicted rupture time for several stresses is given in Table 13.4-IV.

When combined pressure and thermal stresses are considered, Equation 13.4-3 must be solved numerically. For the materials and loadings expected in the TITAN-I first wall during a LOFA, we have found that the thermal stresses have a negligible influence on the rupture time, relative to the pressure stresses, so the results of Table 13.4-IV for pure pressure stresses is used to estimate the rupture and failure times. Table 13.4-IV shows that expected primary stress in the TITAN-I design during a LOFA (2 MPa) would not result in any failure in the first wall.

**Table 13.4-IV.**  
**CREEP-RUPTURE TIME FOR TITAN-I FIRST WALL**

| Primary Stress, $\sigma_p$ (MPa) | Rupture Time, $t_r$ (h) |
|----------------------------------|-------------------------|
| 10                               | 3200                    |
| 20                               | 360                     |
| 30                               | 101                     |
| 40                               | 41                      |
| 50                               | 20                      |

In some cases, depending on the fracture mode, irradiation can reduce the creep-rupture strain (ductility). In 316 SS for instance, intergranular fracture which occurs at high temperature (811-922 °C), and transgranular fracture which occurs at lower temperatures, are affected differently by neutron damage. Irradiation produces helium which migrates to the grain boundaries and reduces the intergranular fracture strength. Therefore, irradiation of 316 SS decreases the strain to failure in the high temperature (intergranular fracture) regime from > 8% to ~ 2%, but irradiation does not affect the transgranular fracture ductility [20]. In vanadium, intergranular fracture has not been observed [16], even for long rupture times, so irradiation may reduce the creep ductility in all temperature regimes to a few percent. Without specific data it is impossible to estimate the rupture time of an irradiated first wall, but if the ductility is not reduced below 1% to 2%, the thermal stresses will still be incapable of producing rupture, according to the arguments put forth previously.

The decrease in the rupture time for primary stresses is more difficult to estimate. In 316 SS, the rupture time, for a given stress and temperature, is reduced by about an order of magnitude after irradiation of  $9.1 \times 10^{22}$  n/cm<sup>2</sup> [21], which corresponds to about 40 dpa. A similar reduction in vanadium would still not be a problem for primary stresses of 2 MPa expected during a LOFA. Hence, creep rupture is still not expected to occur in the TITAN-I first wall or blanket during a LOFA, even after significant irradiation.

#### 13.4.4. Conclusions

The thermal analysis indicates that the TITAN-I first wall will exceed the prescribed temperature limits during a complete LOCA. As a result, the primary-lithium piping arrangement has been chosen so that a complete LOCA is improbable. A complete LOCA is one in which the entire primary loop, including the torus, is drained of coolant. The worst-case accident scenario is then a double-ended pipe break which spills all of the lithium in the primary loop that is above the height of the break. The 30-s residence time of the lithium on the floor and the ensuing lithium fire compound the consequences. The reactor torus, being the lowest point in the primary loop, remains filled with lithium. Therefore, LOFA conditions within the torus are the governing heat-transfer mechanisms.

During the LOFA (and a lithium fire) the first-wall temperature rises to 990°C, about 300°C above the normal, full-power condition. This moderate temperature excursion occurs because of the low level of afterheat in the vanadium alloy (V-3Ti-1Si), the exclusive use of this alloy throughout the torus assembly, and the heat capacity of the static lithium. The peak temperature is well within the limits for both structural integrity and safety. The hydrostatic pressure of the static lithium during a pure LOFA is not sufficient to overstress the blanket and lead to thermal creep-induced rupture and, hence, LOCA conditions in the reactor torus.

In the TITAN-I design, all of the primary-coolant routings and connections are above the FPC, eliminating the possibility of a credible complete LOCA. The worst local LOCA scenario envisioned for the TITAN-I design is a complete LOCA in the first-wall circuit and a LOFA in the blanket circuit. The thermal response of the FPC is found to be very similar to that of a complete LOFA. Therefore, a partial LOCA in the TITAN-I design would not result in safety concerns.

Higher afterheat is expected in the tungsten plate of the divertor. During a LOFA, the peak temperature in the divertor vanadium cooling tube is 1117°C. This may result in shortening the lifetime of the divertor modules, but failure that would lead to a LOCA is unlikely.

### 13.5. LITHIUM-FIRE ACCIDENTS

The use of high-temperature liquid-lithium as the primary coolant of TITAN-I results in LOFA and LOCA scenarios that are somewhat different from those of water- and gas-cooled systems. The principle difference is the possibility of a lithium spill leading to a

lithium fire. Unless safety features are implemented, the energy content of the lithium fire will contribute significantly to the peak temperature of the torus assembly. The reactor has to be designed to (1) ensure that a lithium fire would be a low probability event, and (2) minimize the consequences of lithium fire should it occur.

The consequences of a lithium fire are slight for the TITAN-I design because of the use of floor drains and drain tanks in the confinement building and vacuum tank. Following the design guidelines of Section 13.3.1, three barriers exist between the primary lithium coolant and air. These barriers are the primary-coolant pipes, the vacuum tank, and the confinement building, as shown in Figure 13.3-1. To further reduce the probability of a lithium fire, argon cover gas is used in the confinement building as presented in Section 13.3.4. In addition, in order to reduce the consequences of a lithium spill, two sets of lithium-drain tanks are used: one set connected to the vacuum tank and one set to the confinement building. These drain tanks are designed such that the complete inventory of lithium can be drained to either tank system in  $< 30$  s (Section 13.3.3). This fast draining design has significant impact on minimizing the consequences of major lithium-fire accidents.

Based on the TITAN-I configuration illustrated in Figure 13.3-2, the consequences of three different lithium-fire scenarios were evaluated. These scenarios differ by their initial conditions. Scenario 1: the confinement building is filled with air and the vacuum tank with argon, and air will enter and argon will leave the vacuum-tank through an  $0.4\text{-m}^2$  opening (corresponding to the total cross-sectional area of two primary-coolant pipes). This scenario is a credible major accident when a double-ended primary-pipe break occurs on the vacuum tank and the argon cover gas flows in and fills the vacuum tank. Also, it is assumed that the confinement building has failed and the air will enter into the confinement building and then diffuse into the vacuum tank.

Scenario 2: the confinement building is filled with air and the vacuum tank is in vacuum, with air flowing in through a  $0.4\text{-m}^2$  hole into the vacuum tank. This scenario is possible, but is less likely than the first scenario. This scenario corresponds to a case where the confinement building cover gas is completely replaced by air because of a major explosion or projectile penetration (*e.g.*, aircraft penetration). Scenario 3: the confinement building and the vacuum tank both are filled with air (worst case). This scenario is not considered a credible accident, since both the confinement building and the vacuum tank would need to be penetrated at the same time and the argon cover gas to be blown away.

The above three lithium-fire accidents were analyzed with the LITFIRE code [22]. A two-cell model, which includes the vacuum tank and the confinement building, was used

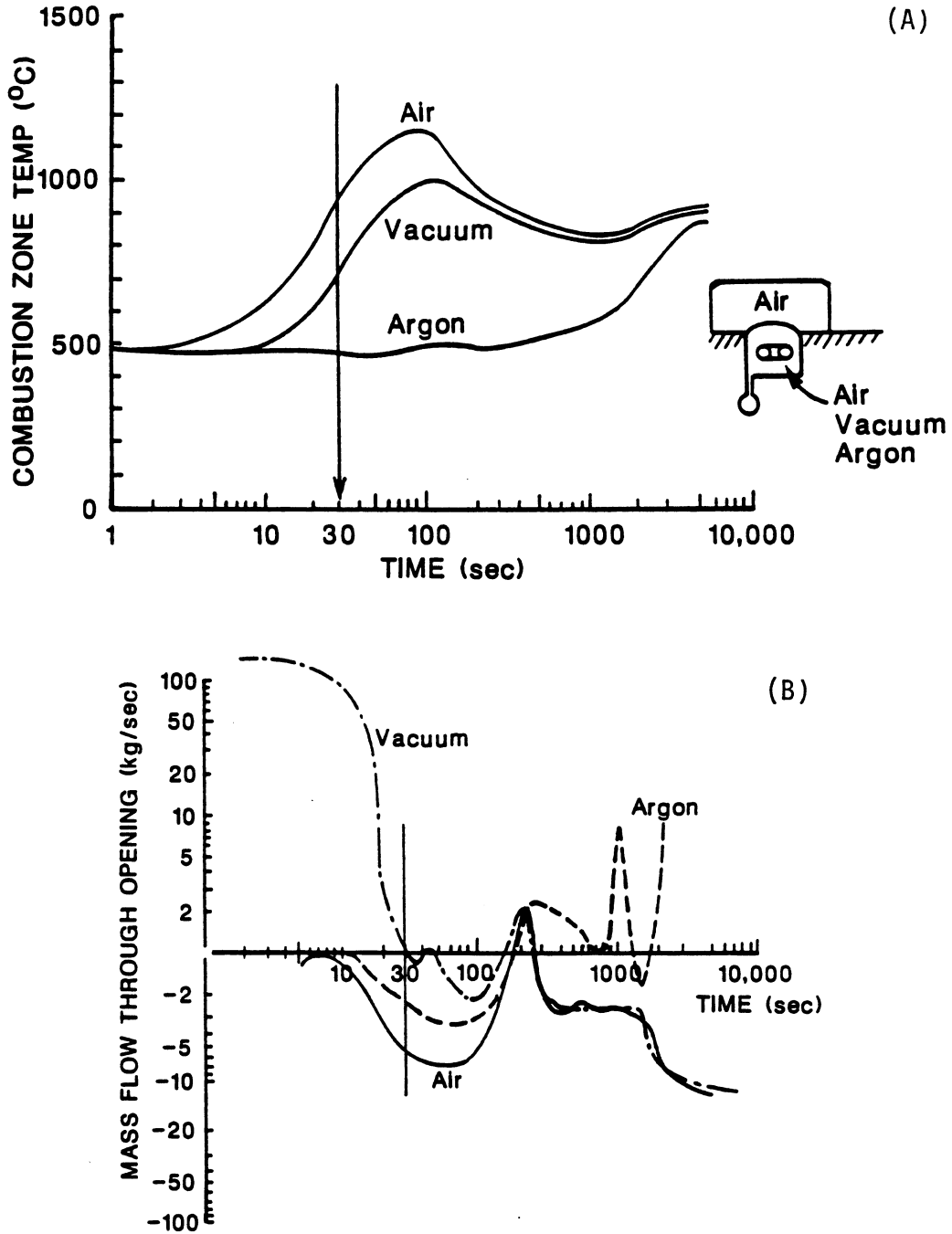
in the calculations. It is assumed that the entire primary-loop inventory of 212 tonne is spilled into the vacuum tank for our worst-case calculations. Other assumptions made in the calculations are: a 5-cm-thick vacuum-tank wall, a 1-mm-thick stainless-steel liner on the floor of the confinement building, and an initial lithium temperature of 495 °C (mixed-lithium operating temperature).

Figure 13.5-1 shows the temperature response of the combustion zone and the mass-flow rate of the opening in the vacuum tank as a function of time, for the three scenarios. For scenario 1 ("Argon"), the vacuum tank is initially filled with argon gas, but the gradual influx of air into the vacuum tank (Figure 13.5-1) initiates the lithium fire and the temperature increases with time. For scenario 2 ("Vacuum"), the vacuum tank is initially in vacuum and air would flow into the tank at the beginning and start the lithium fire. As the lithium fire intensifies, the mass flow through the vessel opening actually reverses and becomes an outward flow (Figure 13.5-1). For scenario 3 ("Air"), the vacuum tank is initially filled with air. The temperature of the combustion zone rises with time until the burning rate is so high that more gas (air and combustion products) is driven out of the vessel than there is air coming in. At this point, the lithium combustion-rate decreases (not enough air) resulting in a decrease in the combustion-zone temperature (Figure 13.5-1). The maximum combustion-zone temperatures are found to be less than 500, 750, and 1000 °C, respectively, for the cases of argon-, vacuum-, and air-filled vacuum tank initial conditions.

Figure 13.5-2 shows the combustion-zone temperature for accident scenario 2 (vacuum tank in vacuum) as a function of time, for different tank-opening sizes and different masses of spilled lithium. It is evident that the combustion-zone temperature is not very sensitive to the opening sizes considered. Also, as the quantity of lithium dumped instantaneously into the vacuum tank is reduced, the maximum combustion-zone temperature is much reduced.

For the three scenarios, it was found that the maximum amount of burned lithium would be 1.6 kg. At a tritium concentration of 1 appm in the lithium coolant of the primary circuit, the maximum release of tritium in this accident is  $6.1 \times 10^{-3}$  g, which is well below the accidental release limit of 200 g [23] to cause a site-boundary dose of less than 25 rem. It should be also be noted that when air is in contact with the hot vanadium structure,  $V_2O_5$  is formed which melts at 670 °C [24]. This can lead to the release of radioactivity from the first-wall and blanket structure. The significance of this reaction and subsequent release of radionuclides should be evaluated.

It can be concluded that under the perceived worst-accident condition of having the vacuum tank initially filled with vacuum, the maximum lithium combustion-zone



**Figure 13.5-1.** The combustion-zone temperature (A) and the mass-flow rate through the opening in the vacuum tank (B) of TITAN-I as a function of time after the lithium spill for the three different accident scenario: the vacuum tank is filled with argon, in vacuum, and filled with air. The confinement building is assumed to be filled with air.

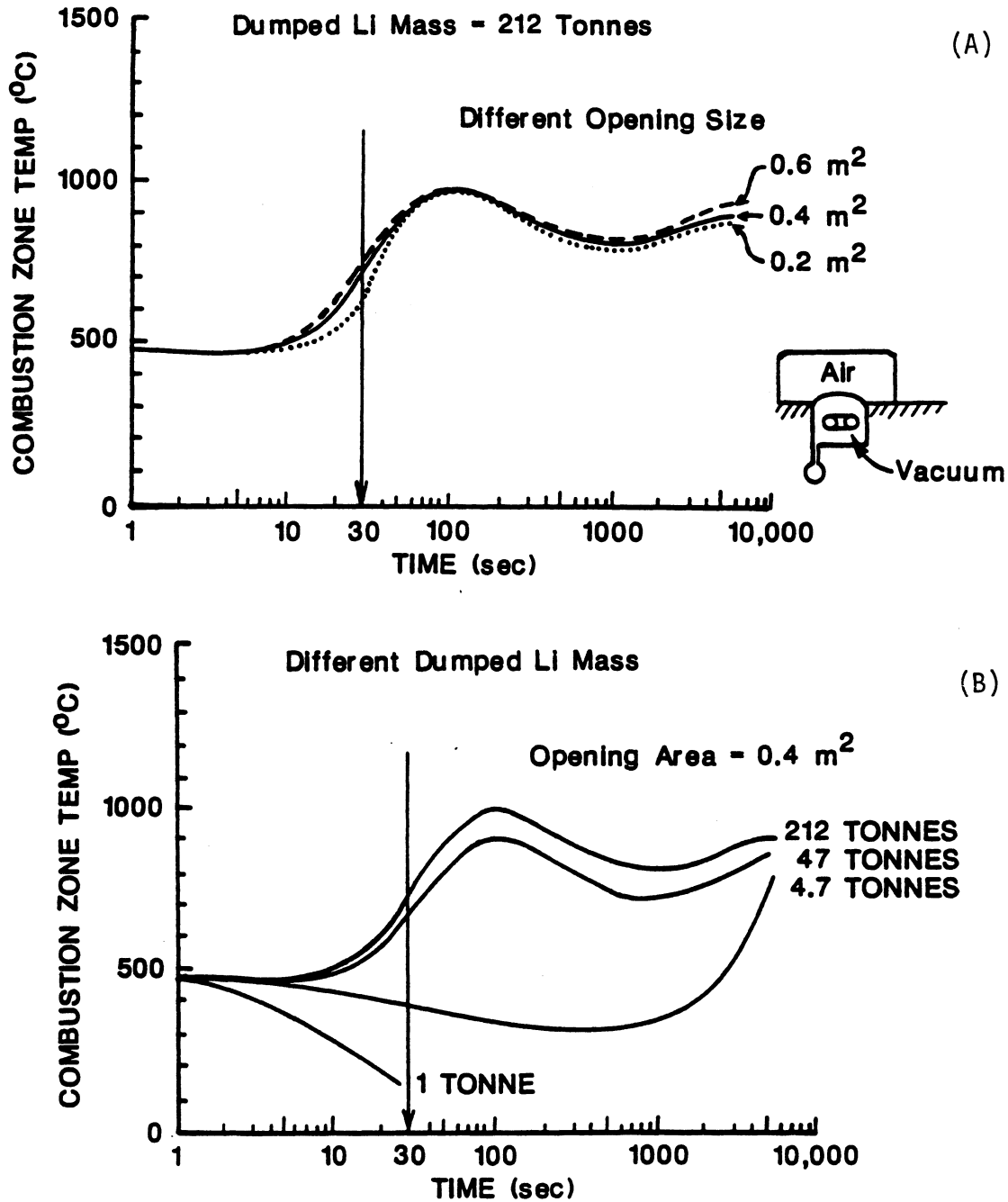


Figure 13.5-2. The combustion-zone temperature of a lithium spill in TITAN-I as a function of time after the spill for different opening sizes in the vacuum tank (A) and different masses of spilled lithium in the vacuum tank (B). The tank is initially in vacuum.

temperature will be  $< 1000^\circ\text{C}$ . Considering the built-in safety feature of the drain tank (drainage of all lithium within 30 s), the maximum temperature can actually be controlled to  $< 750^\circ\text{C}$ , which is within the reuse temperature limits of the structural materials of vanadium, stainless steel, or ferritic steel.

## 13.6. PLASMA ACCIDENTS

In RFPs and tokamaks, in addition to the plasma thermal energy, a significant amount of energy is stored in the poloidal magnetic field. At full operational conditions, the stored energy in TITAN-I plasma includes 0.1 GJ of kinetic (thermal) energy and  $W_M \sim 4.3$  GJ of magnetic energy ( $\sim 5.2$  GJ for ohmic-heating coils in full forward bias). The magnetic energies internal to the plasma are 0.3 MJ in the toroidal field and 0.4 GJ in the poloidal field. The magnetic energies outside the plasma are  $< 2$  MJ in the toroidal field and 3.6 GJ in the poloidal field. Any rapid release of these stored energies (*e.g.*, similar to disruptions in tokamaks) may lead to severe consequences.

Operating RFP experiments usually end with a “current termination” phase where the plasma current is rapidly reduced to approximately zero. Current termination is characterized by the loss of toroidal-field reversal and is accompanied by a positive voltage spike (as opposed to a negative voltage spike for tokamak disruptions) and large density and magnetic-field fluctuations. A number of variables, such as plasma density, toroidal-field reversal, magnetic-field errors, and impurities appear to affect RFP terminations. A complete and satisfactory explanation of RFP current terminations is not yet available. Evidence, however, suggests that the onset of termination may be related to a loss of density possibly leading to a streaming parameter that exceeds a critical value for runaway electrons. Since the value of streaming parameter for TITAN plasma is only a percent of the critical value for runaway electrons, a current termination is not expected during normal, steady-state operation of the TITAN reactor, rather only failure of plasma support technologies leading to an uncontrolled ramp-down of the plasma current will result in a current termination.

A method of controlled current ramp-down has been tested on the HBTX1B experiment in which the toroidal-field-coil circuit is controlled so that the pinch parameter (and the field reversal) is maintained at a given value as the current is decreased to a relatively low level [25]. Maintaining the field reversal in this way is found to delay termination, and the current can be reduced to between 10% to 20% of the maximum value (and the stored magnetic field energy reduced to 1% to 4% of the maximum value) before the

termination occurs. Controlled ramp-downs of this kind forestall the loss of toroidal-field reversal as long as possible and are required for the reactor.

During normal, steady-state operation of the TITAN reactors, the following plasma support technologies are operational: (1) fueling, (2) current-drive, (3) toroidal-field, (4) divertor-field, and (5) equilibrium-field systems. Consequences of failure of each of these systems are discussed below.

**Fueling system.** The effective particle confinement time in the TITAN plasma is very long (a few seconds) because of the operation with high-recycling divertors. The standard shutdown scenario envisioned for the TITAN plasma starts with the termination of plasma fueling and current divertor operations. Therefore, the loss of fueling system (and vacuum pumping) will not initiate an accident and the standard plasma shutdown scenario will be implemented.

**Current-drive system.** Once the current drive fails, the plasma current will resistively decay with time scales of  $L_p/R_p \simeq 200$  to 400 s. As for the case of the failure of the fueling system, the standard plasma shutdown scenario can be implemented here which will prevent any accidents.

**Toroidal-field system.** The toroidal-field (TF) coils provide the reversed toroidal field at the plasma edge. If the TF-coil system (power supplies) fail, the RFP dynamo activity would increase to generate the necessary toroidal flux, resulting in a decay of the plasma current. An emergency plasma shutdown is recommended in this case even though the decay time for the plasma current is probably long enough that a standard shutdown would be possible.

**Divertor-field system.** The TITAN reactors operate with three toroidal-field divertors. If any of the divertor coils fail, the reactor can still be operated at reduced power levels. Failure of all three divertors will result in the plasma "riding" on the first wall in a limiter mode. Since the first wall is designed to handle about 95% of the plasma heat flux (if distributed uniformly on the first wall), a standard shutdown process probably suffices to avert any accidents.

**Equilibrium-field system.** The TITAN reactors use two sets of equilibrium-field (EF) coils: (1) a pair of superconducting magnets provide the main equilibrium field, and (2) a pair of small normal-conducting “trim” coils provide the exact equilibrium (for feedback control of plasma position and for OFCD cycles). With a loss of control on plasma equilibrium and position, not only can the plasma energy be deposited locally, but also the plasma current will decrease rapidly, usually leading to a disruption or current termination. The failure of the equilibrium-field system, therefore, appears to be the most severe plasma-related accident for the TITAN reactor (and for any current-carrying toroidal system).

### 13.6.1. Shutdown Procedures

The TITAN plasma shutdown procedures are guided by the above observations to ensure (1) plasma current is reduced through a controlled ramp-down in order to forestall current termination, (2) plasma equilibrium is maintained during current ramp-down, (3) failure of the equilibrium-field system (*i.e.*, quench of the superconducting EF coils) will automatically lead to an emergency shutdown, and (4) most of the magnetic energy stored in the plasma is removed during the shutdown.

The plasma shutdown scenarios envisioned for the TITAN plasma, therefore, start with termination of fueling and current-drive operations and simultaneous discharge of the EF coils. For the standard shutdown procedure, the duration of the EF-coil discharge can be of the order of a few to tens of seconds. During the emergency shutdown procedure, however, the EF coils are discharged rapidly ( $\sim 0.1$  s) through a resistor which can be combined with the quench protection system for the EF coils. Therefore, failure of the equilibrium-field system will automatically initiate the emergency shutdown procedure.

Because of the strong magnetic coupling between the plasma and EF and OH coils in TITAN, a fast discharge of the EF coils results in a rapid decrease in the plasma current. The parameters of EF and OH circuits, however, are chosen such that the plasma equilibrium is approximately maintained during this discharge without any need for an equilibrium-control system. The large time constant of the IBC TF coils for field penetration is also utilized to ensure maintenance of the field-reversal during the shutdown similar to the controlled current ramp-down technique. Preliminary simulations of the TITAN emergency shutdown procedure (Section 6) indicate that most of the stored magnetic energy (4 to 5 GJ) is removed from the system and dumped through the discharge resistor. Only about 200 MJ of energy is transferred to the first wall in a time scale of

50 to 100 ms, resulting in an average temperature rise in the first wall of about 300 °C; failure of the first wall is not expected.

Despite these favorable results, the RFP theoretical and experimental data base is not very extensive. In particular, no experimental data on high-current, high-temperature, diverted RFP plasmas exist. Furthermore, a complete and satisfactory explanation of current termination in RFPs is not yet available. The safety impact of plasma accidents, therefore, should be further investigated and the shutdown procedures, such as those envisioned for the TITAN plasma, should be experimentally explored.

## 13.7. RADIOACTIVE-WASTE DISPOSAL

### 13.7.1. Radioactive-Waste-Disposal Issues

The classification of nuclear waste for disposal is given under the Code of Federal Regulations, specifically 10CFR61 [1]. Four waste classes have been defined: Class A (segregated waste), Class B (stable waste), Class C (intruder waste), and geologic waste. The first three classes of waste are eligible for near-surface burial, while the last class needs deep geologic burial. Radionuclides with half-lives less than five years will decay by at least six orders of magnitude in 100 years after disposal. These radionuclides can be reasonably managed to meet either Class-A or Class-B disposal requirements. For long-lived radionuclides with half-lives greater than 100 years, however, it will be difficult to meet either Class-A or Class-B disposal requirements solely by radioactive decay to reduce the activity level. To qualify as Class-C or better nuclear waste, the nuclear components in a fusion reactor should minimize the quantity of their alloying and/or impurity elements that would produce long-lived radionuclides.

The limiting-specific activities for near-surface (Class A, B, and C) disposal of nuclear waste were also specified in 10CFR61 regulations for the following radionuclides:  $^{59}\text{Ni}$ ,  $^{94}\text{Nb}$ ,  $^{99}\text{Tc}$ ,  $^{129}\text{I}$ ,  $^{90}\text{Sr}$ ,  $^{137}\text{Cs}$ , and alpha-emitting transuranic nuclides with half-lives greater than five years. These limiting-specific activities were given primarily for radionuclides relevant to present-day applications such as fission-based nuclear reactors. Many radionuclides with half-lives greater than five years, such as  $^{42}\text{Ar}$  (half-life 33 y),  $^{108m}\text{Ag}$  (127 y), and  $^{186m}\text{Re}$  ( $2 \times 10^5$  y), may be produced by fusion reactors in the elements constituting the structural alloy (*e.g.*, vanadium), the divertor collecting plates (*e.g.*, tungsten), and impurities in the structural alloys. However, the limiting-specific activities for near-surface disposal of nuclear waste containing these nuclides are not available in 10CFR61.

Evaluations of limiting-specific activities for fusion-relevant nuclides were made based on 10CFR61 values. A complete work was recently performed by Fetter [26] providing limiting-specific activities for near-surface disposal of all radionuclides with atomic numbers less than 84. These evaluations, consistent in methodology with the 10CFR61 regulations, were used in the waste-disposal analysis of the TITAN-I reactor. Note that discrepancies may exist between Fetter's evaluations and 10CFR61 or other estimates. The major discrepancy occurs with the nuclide  $^{63}\text{Ni}$  for which Fetter's evaluation of the allowable limiting-specific activity is greater than the 10CFR61 limit by more than two orders of magnitude. Also, several nuclides are not given by 10CFR61 evaluations or other estimates:  $^{39}\text{Ar}$ ,  $^{152}\text{Eu}$ ,  $^{192m}\text{Ir}$ ,  $^{137}\text{La}$ ,  $^{186m}\text{Re}$ ,  $^{121m}\text{Sn}$ , and  $^{158}\text{Tb}$ . These nuclides are now covered by Fetter's evaluations. Comparison of these evaluations and resolution of any discrepancies should be carried out as the development of fusion-energy technologies progresses.

### 13.7.2. Radioactive-Waste-Disposal Ratings of TITAN-I Reactor

The neutron spectrum at the first wall, IBC, shield, and ohmic-heating (OH) coils of the TITAN-I design are given in Table 13.7-I. The fast-neutron fraction of the spectrum decreases in the shield and magnets because of enhanced neutron moderation. The increase of the relative low-energy neutron population in these components will result in a higher production rate of long-lived radionuclides such as  $^{94}\text{Nb}$  which depend on  $(n,\gamma)$  reactions.

The neutron fluxes calculated for the reference TITAN-I reactor were used as the input to the activation calculation code, REAC [27]. These results were analyzed to obtain the allowable concentrations of alloying and impurity elements in the vanadium-alloy structural material of the TITAN-I FPC (with a number density of  $7.22 \times 10^{22}$  atoms/cm<sup>3</sup>), and in the OH magnets. At any locations in the TITAN-I FPC, the reaction products of the two main alloying elements in the V-3Ti-1Si alloy (vanadium and titanium) would have no limits on their concentrations to qualify as Class-C waste. The other alloying element, silicon, also poses no problem for the Class-C disposal of the vanadium alloy since its allowable concentration (23%) is much more than needed in this alloy (1%).

The allowable concentrations of various impurities in the vanadium structural material of the TITAN-I reactor are listed in Table 13.7-II. The impurity elements and their levels in V-3Ti-1Si alloy are not specifically given in the literature. The information compiled in Reference [9] for V-15Cr-5Ti was used for comparison in this study and is also noted in Table 13.7-II which shows that Nb (4-appm nominal concentration [9]) is probably the

**Table 13.7-I.**  
**NEUTRON SPECTRUM IN THE TITAN-I FPC**

| Component <sup>(a)</sup> | Neutron Flux<br>(n/cm <sup>2</sup> ) | Flux-Reduction<br>Factor <sup>(b)</sup> | Fast-Neutron<br>Fraction <sup>(c)</sup> |
|--------------------------|--------------------------------------|---|---|
| First wall & IBC         | $4.4 \times 10^{15}$                 | -                                       | 82%                                     |
| Hot shield (zone 1)      | $1.5 \times 10^{15}$                 | 2.9                                     | 70%                                     |
| Hot shield (zone 2)      | $4.6 \times 10^{14}$                 | 3.3                                     | 52%                                     |
| OH coils                 | $1.7 \times 10^{14}$                 | 2.7                                     | 43%                                     |

(a) Flux values at the front side of each component.

(b) Ratio of flux in the front of the component to that in the back.

(c) For  $E_n \geq 0.1$  MeV.

only impurity element that has to be controlled for the shield to qualify as Class-C waste. Also, the allowable impurity concentrations of Nb in the shield ( $\sim 1$  appm) and in the first wall and blanket ( $\sim 5$  appm) are lower than the Nb impurity levels cited in Reference [9]. Certain elements that are not listed in Reference [9] but require strict concentration limits (1 appm or less) for Class-C disposal are Ag, Ir, and Tb. Table 13.7-II indicates that with the nominal impurity levels, the Tb and Ir concentrations in the first wall, blanket, and shield of the TITAN-I reactor may exceed the limit for Class-C disposal. Therefore, special attention should be given to controlling the concentration of these impurity elements.

Because of the low-sputtering and high-temperature properties, tungsten divertor plates are used. The allowable concentration of tungsten in the divertor plates, located mostly close to the plasma, is about 5% (Table 13.7-II). If the divertor plates of the TITAN-I design are disposed of as a unit (mixing the tungsten armor with the vanadium-alloy cooling tubes of the divertor plate), the tungsten concentration in the divertor plates is about 50%, thus giving a factor of 10 higher than the limit for Class-C waste disposal. However, the quantity in this category (non-Class C or geologic) to be disposed annually is small ( $\sim 0.35$  tonne or  $\sim 0.03$  m<sup>3</sup> by volume). Except for the divertor plates, all other

TITAN-I components are classified as Class-C or better nuclear waste if the impurity elements (mainly niobium) are controlled below the allowable limits.

Table 13.7-III summarizes the TITAN materials and related quantities for Class-C disposal. As shown in Table 13.7-III, the total weight of TITAN-I FPC is  $\sim 1363$  tonne. The weight of the magnet system (OH and equilibrium-field (EF) coils, and EF shield) is  $\sim 73\%$  of the total weight of the FPC. The magnet system has a 30-FPY lifetime and disposal (or recycling) is needed only at decommissioning of the power plant. The

Table 13.7-II.

**MAXIMUM CONCENTRATION LEVELS<sup>(a)</sup> OF IMPURITIES IN  
TITAN-I REACTOR COMPONENTS TO QUALIFY AS CLASS-C  
WASTE**

| Element | Major Nuclide<br>(Activity Limit) <sup>(b)</sup>                                       | Components                             |                                      |                                     | Nominal<br>Level |
|---------|--|--|--------------------------------------|-------------------------------------|------------------|
|         |  | FW & Blanket<br>(1 FPY) <sup>(c)</sup> | Hot Shield<br>(5 FPY) <sup>(c)</sup> | OH Coils<br>(30 FPY) <sup>(c)</sup> |                  |
| Nb      | <sup>94</sup> Nb (0.2 Ci/m <sup>3</sup> )  | 5.                                     | 1.4                                  | 0.5                                 | 0.1              |
| Mo      | <sup>99</sup> Tc (0.2 Ci/m <sup>3</sup> )<br><sup>94</sup> Nb (0.2 Ci/m <sup>3</sup> ) | 65.                                    | 100.                                 | 90.                                 | 1.0              |
| Ag      | <sup>108m</sup> Ag (3 Ci/m <sup>3</sup> )  | 1.3                                    | 1.5                                  | 0.7                                 | 1.0              |
| Tb      | <sup>158</sup> Tb (4 Ci/m <sup>3</sup> )   | 0.4                                    | 0.6                                  | 7.0                                 | 5.0              |
| Ir      | <sup>192m</sup> Ir (2 Ci/m <sup>3</sup> )  | 0.1                                    | 0.1                                  | 0.02                                | 5.0              |
| W       | <sup>186m</sup> Re (9 Ci/m <sup>3</sup> )  | 5%                                     | 9%                                   | 100%                                | 0.89%            |

(a) Concentrations in appm except as noted.

(b) From Reference [27].

(c) Based on operation at 18 MW/m<sup>2</sup> of neutron wall loading.

Table 13.7-III.

**SUMMARY OF TITAN-I REACTOR MATERIALS AND RELATED  
WASTE QUANTITIES FOR CLASS-C WASTE DISPOSAL**

| Component           | Material         | Lifetime<br>(FPY) <sup>(a)</sup> | Volume<br>(m <sup>3</sup> ) | Weight<br>(tonne) | Annual                          |
|---------------------|------------------|----------------------------------|-----------------------------|-------------------|---------------------------------|
|                     |                  |                                  |                             |                   | Replacement<br>Mass (tonne/FPY) |
| First wall          | V-3Ti-1Si        | 1                                | 0.4                         | 2.5               | 2.5                             |
| Blanket (IBC)       | V-3Ti-1Si        | 1                                | 6.4                         | 39.2              | 39.2                            |
| Shield (zone 1)     | V-3Ti-1Si        | 5                                | 15.5                        | 95.6              | 19.1                            |
| Shield (zone 2)     | V-3Ti-1Si        | 5                                | 28.0                        | 172.0             | 34.4                            |
| OH coils            | Modified steel   | 30                               | 3.8                         | 34.0              | 1.1                             |
|                     | Copper           |                                  | 26.6                        | 239.0             | 8.0                             |
|                     | Spinel           |                                  | 3.8                         | 15.2              | 0.5                             |
|                     | TOTAL            |                                  | 34.2                        | 289.2             | 9.6                             |
| EF coils            | Modified steel   | 30                               | 43.0                        | 315.0             | 10.5                            |
| EF shield           | Modified steel   | 30                               | 43.9                        | 347.0             | 11.6                            |
|                     | B <sub>4</sub> C |                                  | 18.8                        | 47.0              | 1.6                             |
|                     | TOTAL            |                                  | 62.7                        | 394.0             | 13.2                            |
| Divertor shield     |                  |                                  |                             |                   |                                 |
| zone 1              | V-3Ti-1Si        | 1                                | 2.3                         | 14.2              | 14.2                            |
| zone 2              | V-3Ti-1Si        | 5                                | 6.7                         | 41.2              | 8.2                             |
| TOTAL CLASS-C WASTE |                  |                                  | 199.                        | 1363.             | 151.                            |

(a) Based on operation at 18 MW/m<sup>2</sup> of neutron wall loading.

components to be replaced annually are first wall, blanket, and front part of the divertor shield, and constitute only 4% of the total weight of the FPC. The balance of the weight is contributed by the 5-FPY-lifetime components (*i.e.*, hot shield and the rear part of the divertor shield). The average annual-replacement mass of the FPC is about 150 tonne/FPY (Table 13.7-III).

### 13.7.3. Conclusions

The waste-disposal analysis has shown that the compact, high-power-density TITAN-I reactor can be designed to meet the criteria for Class-C waste disposal. The key features for achieving Class-C waste in the TITAN-I reactor are attributed to: (1) materials selection, and (2) control of impurity elements. The materials selected for the TITAN-I reactor are vanadium alloy (V-3Ti-1Si) and lithium for the FPC. The main alloying elements of these materials do not produce long-lived radionuclides with activity levels exceeding the limits for Class-C disposal. The impurity elements, mainly niobium and possibly silver, terbium, and iridium, need to be controlled in the vanadium alloy below appm levels.

The average replacement mass was estimated to be 150 tonne/FPY ( $\sim 11\%$  of total FPC). The divertor plates are fabricated with a tungsten armor because of its sputtering properties. The waste-disposal rating of the divertor plates is estimated to be a factor of 10 higher than for Class-C disposal after one year operation. The annual disposal mass of this non-Class-C waste is 0.35 tonne/FPY ( $\sim 0.23\%$  of the FPC replacement mass).

The conclusions derived from the TITAN-I reactor study are general, and provide strong indications that Class-C waste disposal can be achieved for other high-power-density approaches to fusion. These conclusions also depend on the acceptance of recent evaluations of limiting-specific activities carried out under 10CFR61 methodologies.

## 13.8. SUMMARY AND CONCLUSIONS

Strong emphasis has been given to safety engineering in the TITAN study. Instead of an add-on safety design and analysis task, the safety activity was incorporated into the process of design selection and integration at the beginning of the study. The safety-design objectives of the TITAN-I design are: (1) to satisfy all safety-design criteria as specified by the U. S. Nuclear Regulatory Commission on accidental releases, occupational doses, and routine effluents; and (2) to aim for the best possible level of passive safety assurance.

The key safety features of the lithium self-cooled TITAN safety design are:

- The selection of a low-afterheat structural material, V-3Ti-1Si;
- The selection of a relatively high  $^6\text{Li}$  enrichment (30%) to aid in further reducing afterheat and radioactive wastes;
- The use of three enclosures separating the lithium and air: the blanket tubes, vacuum vessel, and confinement building which is filled with argon cover gas;
- Locating all coolant piping connections at the top of the torus to prevent a complete loss of coolant in the FPC in case of a pipe break;
- The use of lithium-drain tanks to reduce the vulnerable lithium inventory should a pipe break occur;
- The use of steel liner to cover the confinement-building floor to minimize the probability of lithium-concrete reaction;
- The exclusion of water from the confinement building and vacuum vessel to prevent the possibility of lithium-water reaction.

With the above design features, we found that during LOFA, the first wall temperature rises to a maximum of  $990^\circ\text{C}$ , which is well below the recrystallization temperature of the V-3Ti-1Si alloy. We also found that the hydrostatic pressure of the lithium is not sufficient to over-stress the first wall and blanket and lead to thermal creep-induced rupture. Therefore, it is not expected that a LOFA will lead to a LOCA. Also, a complete LOCA is not credible because all the piping connections are located above the reactor torus.

In the event of major primary-pipe breaks and failure of the confinement building and vacuum vessel, air could enter the vacuum chamber and start a lithium-fire. Drain-tank systems are provided to drain the maximum amount of lithium in less than 30 s, and we found that during the perceived worst-accident condition of a lithium fire, the maximum combustion-zone temperature is less than  $1000^\circ\text{C}$ . The tritium release in this case would be about 60 Ci which is quite acceptable under this worst-accident scenario. A critical concern under the lithium-fire scenario is the formation and release of vanadium oxide,  $\text{V}_2\text{O}_5$ . Further measurement of vanadium-oxide formation and its vapor pressure with temperature, and the calculation of potential releases to the public based on the TITAN-I configuration and accidental scenarios should be performed.

The total tritium inventories in the lithium primary loop and the secondary loop are 344 and 300 g, respectively. These inventories are acceptable when passive drain tanks are used to control the amount of possible tritium releases. The tritium inventory in the blanket structure is less than 10 g, which is also acceptable. The tritium-leakage rate from the primary loop was estimated to be 7 Ci/d which is within the 10 Ci/d design goal.

Plasma-accident scenarios need to be further evaluated as the physics behavior of RFPs becomes better understood. Preliminary results indicate that passive safety features can be incorporated into the design so that the accidental release of plasma and magnetic energies can be distributed without leading to major releases of radioactivity. Activities in this area need to be continued, especially for high-power-density devices.

Based on the analyses summarized above, TITAN-I does not need to rely on any active safety systems to protect the public. A LOFA will result in no radioactive release and will not lead to a more serious LOCA. A complete LOCA from credible events is not possible. Only the assurance of coolant-piping and vacuum-vessel integrity is necessary to protect the public. The TITAN-I design, therefore, meets the definition of level 3 of safety assurance, "small-scale passive safety assurance." Pending information on the vanadium-oxide formation and releases from the TITAN-I vacuum chamber under the lithium-fire accident scenario, the qualification of TITAN-I as a level-2 of safety assurance design, "large-scale passive safety assurance," may also be possible.

**REFERENCES**

- [1] "Standards for Protection Against Radiation," U. S. Nuclear Regulatory Commission, Code of Federal Regulations, Title 10, Part 0 to 199 (1986).
- [2] "Domestic Licensing of Production and Utilization Facilities," U. S. Nuclear Regulatory Commission, Code of Federal Regulations, Title 10, Chapter 1, Part 50 (1984).
- [3] "Reactor Site Criteria," U. S. Nuclear Regulatory Commission, Code of Federal Regulations, Title 10, Chapter 1, Part 100 (1975).
- [4] "Nuclear Safety Criteria for the Design of Stationary Boiling Water Reactor Plants," American Nuclear Society, ANSI/ANS - 52.1 (1983).
- [5] R. E. Tiller, "Proposed Revision of DOE Order 5480.1A, Radiation Standards for Protection of the Public," U.S. Department of Energy Memorandum PE-243 to W. H. Hoover, A. W. Trivelpiece, and J. W. Vaughan (September 17, 1984).
- [6] K. R. Schultz, F. S. Dombek, *et al.*, "Safety Considerations — Field-Reversed Mirror Pilot Reactor," Electric Power Research Institute report EPRI AP-1544 (1980) Part IV, Section 1.
- [7] S. J. Piet, "Approaches to Achieving Inherently Safe Fusion Power Plants," *Fusion Technol.* **10** (1986); also "Inherent/Passive Safety For Fusion," in *Proc. 7th ANS Topical Meeting on Technol. of Fusion Energy*, Reno, NV (1986).
- [8] J. P. Holdren *et al.*, "Summary of the Report of the Senior Committee on Environmental, Safety and Economic Aspects of Magnetic Fusion Energy," Lawrence Livermore National Laboratory report UCRL-53766-Summary (1987); also J. P. Holdren *et al.*, "Exploring the Competitive Potential of Magnetic Fusion Energy: The Interaction of Economics with Safety and Environmental Characteristics," *Fusion Technol.* **13** (1988) 7.
- [9] D. L. Smith *et al.*, "Blanket Comparison and Selection Study, Final Report," Argonne National Laboratory report ANL/FPP-84-1 (1984).
- [10] G. J. Desalvo and J. A. Swanson, "ANSYS User's Manual," Swanson Analysis Systems, Inc. (1979).
- [11] P. J. Burns, "TACO2D - A Finite Element Heat Transfer Code," Lawrence Livermore National Laboratory report UCID-17980, Rev. 2 (1982).

- [12] A. B. Shapiro, "TOPAZ – A Finite Element Heat Conduction Code for Analyzing 2-D Solids," Lawrence Livermore National Laboratory report UCID-20045 (1984).
- [13] I. LeMay, *Principles of Mechanical Metallurgy*, Elsevier, New York (1982) p. 367.
- [14] S. S. Manson and C. R. Ensign, NASA report TM.X-52999 (1971).
- [15] N. M. Ghoniem and R. W. Conn, "Assessment of Ferritic Steels for Steady State Fusion Reactors," *Fusion Reactor Design and Technology II*, International Atomic Energy Agency, IAEA-TC-392-62 (1983) p. 389.
- [16] D. L. Harrod and R. E. Gold, "Mechanical Properties of Vanadium and Vanadium-Base Alloys," Review 255, *Int. Met. Rev.* 4 (1980) 163.
- [17] R. E. Gold and R. Bajaj, "Mechanical Properties of Candidate Vanadium Alloys for Fusion Applications," *J. Nucl. Mater.* 122-123 (1984) 759.
- [18] E. L. Robinson, "Effect of Temperature Variation on the Creep Strength of Steels," *Trans. ASME* 60 (1938) 253.
- [19] M. Bocek, "Creep Rupture at Monotonous Stress and Temperature Ramp Loading: I. Calculations," *J. Nucl. Mater.* 82 (1979) 329.
- [20] C. W. Hunter and G. D. Johnson, "Mechanical Properties of Fast Reactor Fuel Cladding for Transient Analysis, Irradiation Effects on the Microstructure and Properties of Metals," Amer. Soc. Testing and Mater. STP 611 (1976) 101.
- [21] R. L. Fish, "Creep-Rupture Properties of 20% Cold-Worked Type 316 Stainless Steel After High Fluence Neutron Irradiation," *Nucl. Technol.* 35 (1977) 9.
- [22] E. Yachimiak, V. Gilberti, and M. S. Tillack, "LITFIRE User's Guide," Massachusetts Institute of Technology report PFC/RR-83-11 (1983).
- [23] I. Maya and K. R. Schultz, "Final Report, Inertial Confinement Fusion Reaction Chamber and Power Conversion System Study," General Atomics report GA-A17842 (1985).
- [24] R. M. Neilson, Jr., "Volatility of V15Cr55Ti Fusion Reactor Alloy," *J. Nucl. Mater.* 141-143 (1986) 607.
- [25] A. A. Newton and P. G. Noonan, "Controlled Termination of Reversed-Field-Pinch Discharges," *Nucl. Instr. and Methods* A245 (1986) 167.

- [26] S. Fetter, E. T. Cheng, and F. M. Mann, "Long-Term Radioactivity in Fusion Reactors," *Fusion Eng./Des.* **6** (1988) 123.
- [27] F. M. Mann, "Transmutation of Alloys in MFE Facilities as Calculated by REAC (A Computer Code for Activation and Transmutation Calculations)," Hanford Engineering and Development Laboratory report HEDL-TME 81-37 (1982).